

2007

Measurement of interparticle forces between eutectic BaF₂ - CaF₂ particles using atomic force micr

Deepa Balakrishnan
University of Dayton

Follow this and additional works at: https://ecommons.udayton.edu/graduate_theses

Recommended Citation

Balakrishnan, Deepa, "Measurement of interparticle forces between eutectic BaF₂ - CaF₂ particles using atomic force micr" (2007). *Graduate Theses and Dissertations*. 1373.
https://ecommons.udayton.edu/graduate_theses/1373

This Thesis is brought to you for free and open access by the Theses and Dissertations at eCommons. It has been accepted for inclusion in Graduate Theses and Dissertations by an authorized administrator of eCommons. For more information, please contact mschlangen1@udayton.edu, ecommons@udayton.edu.

MEASUREMENT OF INTERPARTICLE FORCES BETWEEN EUTECTIC
BaF₂ - CaF₂ PARTICLES USING ATOMIC FORCE MICROSCOPY

Thesis

Submitted to

The School of Engineering

UNIVERSITY OF DAYTON

In Partial Fulfillment of the Requirements for

The Degree

Master of Science in Chemical Engineering

by

Deepa Balakrishnan

UNIVERSITY OF DAYTON

Dayton, Ohio

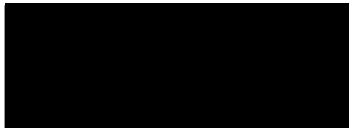
December 2007

Measurement of Interparticle Forces between Eutectic BaF_2 - CaF_2 Particles
Using Atomic Force Microscopy

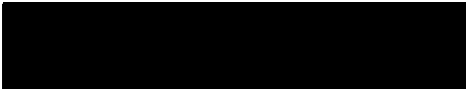
APPROVED BY:



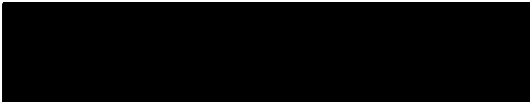
Shamachary Sathish, Ph.D.
Advisory Committee Chairman
Professor, Materials Engineering
Department



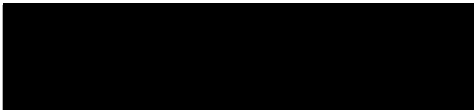
Kevin J. Myers, D.Sc., P.E.
Academic Advisor
Professor, Chemical and Materials
Engineering Department



P. Terrence Murray, Ph.D.
Committee Member
Professor, Materials Engineering
Department



Malcolm K. Stanford, Ph.D.
Committee Member
Visiting Professor, Materials
Engineering Department



Malcolm W. Daniels, Ph.D.
Associate Dean
School of Engineering



Joseph E. Saliba, Ph.D., P.E.
Dean, School of Engineering

ABSTRACT

MEASUREMENT OF INTERPARTICLE FORCES BETWEEN EUTECTIC BaF_2 - CaF_2 PARTICLES USING ATOMIC FORCE MICROSCOPY.

Name: Balakrishnan, Deepa
University of Dayton

Advisor: Dr. Shamachary Sathish

The inter-particle forces between eutectic BaF_2 - CaF_2 powder particles used in solid lubricants [PS304] are affected by the presence of humidity and electrostatic charges. Large inter-particle forces tend to create clogging of the feedstock during the production of solid lubricant coatings. To reduce the clogging and to enhance the smooth formation of solid lubricant coatings there is a need to understand the contribution of humidity and electrostatic forces to the inter-particle forces.

The effect of electrostatic charges on the interparticle forces between spherical particles of eutectic BaF_2 - CaF_2 and substrate of eutectic BaF_2 - CaF_2 have been investigated using an Atomic Force Microscope (AFM). The force measurements were performed with powder particles of eutectic BaF_2 - CaF_2 manufactured by gas atomization. The standard AFM tip was replaced with a spherical particle of eutectic BaF_2 - CaF_2 with probe diameter of 21 μm – 30 μm . The sample substrate of eutectic BaF_2 - CaF_2 was produced by compaction of the

powder particles at high pressure. A static generator was used to produce electrostatic charge on the eutectic $\text{BaF}_2\text{-CaF}_2$ substrate for a fixed potential and for a fixed time. AFM was used to measure the interparticle force between the eutectic $\text{BaF}_2\text{-CaF}_2$ particle and the eutectic $\text{BaF}_2\text{-CaF}_2$ substrate by analyzing the force displacement curves obtained at various locations on the substrate. The effect of electrostatic force on the force curve was studied for different diameter particles. Force measurements were performed at several locations on the substrate to determine the variability. Measurements as a function of the amount of electrostatic charge were compared with measurements performed without charging. Large variation in the electrostatic force was observed for different diameter particle tips. The reasons for the variation in the electrostatic force for different diameter tips and at several locations are explained. From the understanding obtained with the relative strength of the measured electrostatic force, new methods can be developed to avoid the clogging of eutectic $\text{BaF}_2\text{-CaF}_2$ particles.

Although the research project is directed towards application to solid lubricants, interparticle forces are very fundamental to many applications. The understanding gained in this project can be applied in other industries like powder compaction, electrophotography, pharmaceuticals, etc

ACKNOWLEDGEMENTS

Foremost, I would like to express my deepest gratitude to my advisor Dr. Sathish Shamachary. I have been surprisingly fortunate to have an advisor who gave me the freedom to explore on my own and at the same time the guidance to recover when I faltered. This work would not have been possible without his support and encouragement.

My warm thanks to Dr. Malcolm Keith Stanford for providing the samples required for this study and for his suggestions and feedback on my thesis work.

I am grateful to Richard Reibel and Larry Dukate for providing me the electrostatic generator. I wish to thank Jennifer L. Pierce for training me on white light interference microscope.

I would like to acknowledge the NASA Glenn Center, Cleveland, the Department of Chemical and Materials Engineering and the Graduate School for financial support.

My sincere thanks are due to my thesis committee members Dr. Kevin Myers and Dr. P. Terrence Murray for their suggestions and feedback on my thesis. I would like to thank Vijay Nalladega for training me on the AFM instrument and for help on this research project.

TABLE OF CONTENTS

Abstract	iii
Acknowledgements	v
List of Figures	viii
CHAPTER 1 INTRODUCTION	
1.1) Motivation	1
1.2) Force	4
1.2.1) Fundamental Forces	4
1.2.2) Intermolecular / Interparticle Forces	6
1.2.3) Interactive Forces of Powder Particles	11
1.3) Force Measurements	15
1.4) Electrostatic Force Measurements	16
1.4.1) Atomic Force Microscope (AFM)	16
1.5) Significance of Atomic Force Microscope (AFM) in Force Studies	17
1.6) Background	18
CHAPTER 2 INSTRUMENTATION AND EXPERIMENTAL METHOD	
2.1) Introduction	22
2.2) Principle of AFM	23

2.3) Basic AFM Components	24
2.4) Force Curve	31
2.5) Contact Mode	33
2.6) Electrostatic Generator System	35
2.7) Electrostatic Locator	38
2.8) Experiment	39
CHAPTER 3 RESULTS AND DISCUSSION	
3.1) Introduction	42
3.2) Charge-Time Relation of Eutectic BaF ₂ -CaF ₂ Substrate	43
3.3) Effect of Electrostatic Charge on the Force Curve	45
3.4) Time Dependence of Electrostatic Charge on the Force-Distance Curve	49
3.5) Effect of Electrostatic Charge on the Force Curve as a Function of Tip Diameter	51
3.6) Electrostatic Force Measurement at Various Locations on the Substrate	56
3.7) Influence of Particle Roughness on Electrostatic Force Measurement	58
CHAPTER 4 CONCLUSIONS	61
CHAPTER 5 FUTURE RESEARCH.....	63
REFERENCES	64

LIST OF FIGURES

1)	Flow diagram of intermolecular / interparticle forces	10
2)	The Derjaguin approximation which relating the force law F_e between two spheres of equal size	14
3)	SEM images of spherical $BaF_2 - CaF_2$ particles.....	20
4)	Schematic diagram of the working principle of an AFM	24
5)	Basic AFM components	25
6)	Piezoelectric scanner	26
7)	Triangle cantilever of the AFM.....	28
8)	The spherical eutectic $BaF_2 - CaF_2$ particle attached to the tip of the cantilever.....	29
9)	Beam deflection detection method	30
10)	Typical force-distance curve	32
11)	Force – distance curve	34
12)	Electrostatic generator system PN57A with sample substrate.....	37
13)	Typical charging electrode	37
14)	Probe or electrode of PN57A with sample substrate	38
15)	Electrostatic locator SIMCO SS-2X	39
16)	The dissipation of substrate electrostatic charge with time.....	43

17)	The force-distance curve of uncharged eutectic $\text{BaF}_2 - \text{CaF}_2$ substrate	46
18)	The force -distance curve of charged eutectic $\text{BaF}_2 - \text{CaF}_2$ substrate	46
19)	Electrostatic and van der Waals forces	47
20)	Force as a function of distance	48
21)	Time - dependence of electrostatic force on the force- distance curve	50
22)	Time - dependence of electrostatic force on the force -distance curve for different tips	53
23)	Exponential decay of electrostatic force as a function of time for various $\text{BaF}_2\text{-CaF}_2$ tip diameters	54
24)	Electrostatic force for several diameter tips of AFM	55
25)	Electrostatic force at various locations on the substrate.....	57
26)	3-D image showing the asperity of an individual spherical particle of eutectic $\text{BaF}_2\text{-CaF}_2$	58
27)	WLI data of the substrate surface	59
28)	Stitched image of eutectic $\text{BaF}_2\text{-CaF}_2$ substrate	60

CHAPTER 1

INTRODUCTION

1.1) Motivation

Powder flow properties are of great importance in many powder related industries for handling and processing operations, transportation, mixing, compression and packaging. Understanding the nature of various forces acting on fine powder particles is very important in many areas of science and technology. For example, in the semiconductor industry the contamination on wafer surfaces by fine particles is of great concern [1]. In electrophotography, marking the controlled transfer of small charged particles from one surface to another is the key requirement [2]. In the pharmaceutical [3] industry, the adhesion of medicinal particles to specific sites is very important. When the particle sizes are smaller than 1 mm, forces other than that due to gravity dominate, and hence particles are often observed to cling tenaciously to surfaces or to each other. These forces are mostly in the nano - Newton range and strongly depend on atmospheric conditions. The most prominent forces in particle interactions are the adhesive and the cohesive forces. The flow properties are determined by these inter-particle forces (adhesion/cohesion) which are mainly influenced by the van der Waals, capillary and electrostatic

Forces. In order to improve the flow properties, it is necessary to study the interparticle forces qualitatively and quantitatively. Extensive research has been performed over several years to measure the interactive forces between powder particles. Many studies have been conducted on electrophotographic processes for understanding the interactions between powder particles, especially for electrically insulating particles. The dielectric particles naturally acquire charge through the mechanism of triboelectricity by contacting each other or the container walls. The amount of charge on each particle and the distribution of charge among the particles are expected to influence the rheological behavior of a powder.

In the electrophotographic process, charged toner particles are transferred from the bulk to the photoreceptor drum and from there to the paper. Toner transfer from the photoreceptor to the paper is not 100% efficient. Small toner particles and toner with a low charge will have a strong adhesion to the photoreceptor and can remain there after transfer [4]. These particles must be removed from the photoreceptor mechanically or they will affect the printing of the next image. So a fundamental understanding of the electrostatic effect on charged particles is desired. Many research works have been conducted using Atomic Force Microscopy (AFM) to determine the adhesion force between toner particles and substrate. Work is still being done to improve the printing system by determining the electrostatic contribution to the adhesion force, and in understanding particle-particle and particle-substrate interaction. Thus, we can see that there is a need for clear understanding of powder properties which are

determined by inter-particle forces. To enable detailed analysis, the problem needs to be simplified by reducing the number of interacting surfaces. The primary goal of the present study is to determine the interparticle force between spherical particles using Atomic Force Microscope (AFM).

The effect of electrostatic forces on fine particle adhesion appears in our daily life as dirt clinging on clothes and walls. In general, electrostatic forces become important when particle material is electrically insulating so the electric charge can be retained. Electrostatic forces on powder particles arise primarily from the presence of net (or excess) electric charges on the particles or an externally applied electric field. Those dielectric particles naturally acquire charge through the mechanism of triboelectricity by sliding on each other or the container walls. A mathematical evaluation performed by James Q. Feng and Dan A. Hays [5] showed that electrostatic force was greater than the van der Waals force for charged particles. Thus, the effect of electrostatic charge on the interparticle force between two dielectric spheres in contact needs to be addressed in order to understand the material transportation problem [6]. In this discussion, we consider only eutectic $\text{BaF}_2\text{-CaF}_2$ powder particles that are dielectric. $\text{BaF}_2\text{-CaF}_2$ is a constituent of a NASA-developed composite solid lubricant material designated PS304 [7, 8, 9, 10, 11]. Reliable deposition of PS304 as a coating is highly dependent upon the interparticle forces generated by the $\text{BaF}_2\text{-CaF}_2$ constituent. This study is focused on the quantification of the electrostatic forces between $\text{BaF}_2\text{-CaF}_2$ particles. Since AFM is capable of measuring sub nano-Newton forces, it provides a unique method for investigating

electrostatic interactions. Though a number of studies have been carried out using the surface force apparatus technique (SFA) [12, 13] for measuring the interparticle forces and some studies using the osmotic stress method have been reported, the Atomic Force Microscopy (AFM) is widely used as it provides good precision and sensitivity to probe surfaces with molecular resolution.

The primary goal of this present work is to quantitatively measure the contribution of electrostatic charges to the inter-particle forces between spherical particles of eutectic $\text{BaF}_2\text{-CaF}_2$ and a substrate of eutectic $\text{BaF}_2\text{-CaF}_2$ using an Atomic Force Microscope (AFM). In this project, a substrate made of eutectic $\text{BaF}_2 - \text{CaF}_2$ particles compacted at high pressure and AFM cantilevers with attached eutectic $\text{BaF}_2 - \text{CaF}_2$ particle was used to measure the forces. This approach models the real situation in the feedstock used in plasma spray deposition of PS304 solid lubricant coatings.

1.2) Force

1.2.1) Fundamental Forces

Interactions between particles, and the large-scale behavior of matter throughout the Universe, are determined by four fundamental forces. They are the strong and weak nuclear forces, the electromagnetic force and gravitation.

i) Strong Force

This force is a very strong interaction, which binds neutrons and protons together in the cores of atoms and is a short-range force. It acts only over ranges

on the order of 10^{-13} centimeters and is responsible for holding the nuclei of atoms together. It is basically attractive, but can be effectively repulsive in some circumstances.

ii) Weak Force

The weak force is responsible for radioactive decay and neutrino interactions. It has a very short range and, as its name indicates, it is very weak.

iii) Gravitational Force

The gravitational force is weak, but very long ranged. Furthermore, it is always attractive, and acts between any two pieces of matter in the universe since mass is its source. Gravitation is said to follow an inverse square law, as the force is inversely proportional to the square of the distance between the bodies. Since the force of gravitation follows an inverse square law, the force can be depicted as a conservative force field, in which work done in moving a mass from one point to another is independent of the path followed. The gravitation force is the weakest of all fundamental forces but can assume great magnitude, as there are truly massive bodies present in the universe.

iv) Electro-Magnetic Forces

The electromagnetic force determines the ways in which electrically charged particles interact with each other and with magnetic fields. This force can be attractive or repulsive. Like charges (two positive or two negative charges)

repel each other and unlike forces attract each other. The electromagnetic force binds [negatively charged] electrons into their orbital shells, around the positively charged nucleus of an atom. This force holds the atoms together. Electromagnetic forces are the source of all intermolecular interaction that determine the properties of solids, liquids, gases, the behavior of particles in solution, chemical reactions, and the organization of biological structure.

1.2.2) Intermolecular/ Interparticle Forces

Intermolecular forces are the forces of attractions that exist between molecules in a compound. These forces give rise to bonding energies of less than a few kcal/mol and are generally much weaker than covalent bonds. The strength of the intermolecular forces determines the physical properties of the substance. Intermolecular forces can be generally classified into electrostatic forces (ionic bonding), van der Waals forces, and force due to covalent bonding.

1) Electrostatic Forces – Ionic Compounds

The force of interaction between charged particles is said to be an electrostatic force. This obeys Coulomb's Law, which states that the force is proportional to the product of the electric charges and inversely proportional to the square of the distance between them. By Coulomb's law, the electrostatic force F that two charges q_1 and q_2 with a distance r apart exert on each other is given as

$$F = \frac{1}{4\pi\epsilon_0} \frac{q_1 q_2}{r^2}.$$

The force acts in a straight line connecting the two electric charges, and the force is repulsive when q_1 and q_2 are both positive or both negative, corresponding to a positive value of $q_1 q_2$. The forces are attractive when the charges are opposite of each other so that $q_1 q_2$ is negative. The quantity ϵ_0 is the permittivity constant which is equal to 8.854×10^{-12} coulomb²/ (Newton- meter²). Intermolecular Forces are longest-ranged (act strongly over a large distance) when they are electrostatic. Interaction of Charge Monopoles (simple charges) is the longest-range electrostatic force. Electrostatic forces are categorized by the symmetry of the partners involved in the interactions and are given by the first non-zero moment of the charge distribution, i.e. Monopole, Dipole, Quadrupole, etc. Electrostatic forces only exist between molecules with permanent moments of their charge distribution. Molecules do not have to distort or fluctuate in order to exhibit electrostatic intermolecular forces. The forces between ions and ion-dipole are considered to be electrostatic forces.

Ionic Bonding

i) Charge – Charge Forces

Charge – charge forces are interaction between charged ions. There are two types of electrically charged ions: those which contain more protons than electrons and are said to be positively charged and those which contain more electrons than protons are said to be negatively charged. For like charges (+, +)

or $(-, -)$, this force is always repulsive. For unlike charges $(+, -)$, this force is always attractive. For simple charges, this force follows Coulomb's law.

ii) Ion – Dipole Forces

This force involves an interaction between a charged ion and a polar molecule (a molecule with a dipole). Cations are attracted to the negative end of a dipole. Anions are attracted to the positive end of a dipole. The magnitude of the interaction energy depends upon the charge of the ion, the dipole moment of the molecule and the distance from the center of the ion to the midpoint of the dipole. Ion-dipole forces are important in solutions of ionic substances in polar solvents.

2) Van der Waals Forces

Van der Waals forces are found in non – polar molecules. Van der Waals forces exist in three different levels of strength. The differing strengths are a function of the magnitude of the areas of charge that hold them together. These three different forces are

- Dipole-Dipole Forces
- London Dispersion Forces
- Hydrogen Bonding Forces

i) Dipole – Dipole Forces

These forces exist between neutral polar molecules. Polar molecules attract one another when the partial positive charge on the molecule is near the

partial negative charge on the other molecule. The polar molecules must be in close proximity for the dipole – dipole forces to be large. These forces are characteristically weaker than ion-dipole forces. They increase with increasing polarity of the molecule.

ii) London Dispersion Forces

The London dispersion force is the weakest intermolecular force. In non-polar molecules, the electrons are evenly distributed on either side of the nucleus, but occasionally one side will gain a small excess of electron density. This brief unsymmetrical distribution of electrons gives the atom a dipole moment. When a neighboring atom approaches, it would be influenced which will induces a temporary dipole, resulting in weak attraction forces between the atoms.

iii) Hydrogen Bonding

Hydrogen bonding force is considered to be the strongest force. A hydrogen bond is the attractive force between the hydrogen attached to an electronegative atom of one molecule and an electronegative atom of a different molecule. Usually the electronegative atom is oxygen, nitrogen, or fluorine, which has a partial negative charge. The hydrogen then has the partial positive charge. A polar bond is formed between hydrogen and an electronegative atom such as F, O, or N. The hydrogen atom has no inner core of electrons, so the side of the atom facing away from the bond represents a virtually bare nucleus. This positive charge is attracted to the negative charge of an electronegative atom in a nearby molecule. Because the hydrogen atom in a polar bond is electron- deficient on

one side, this side of the hydrogen atom can get close to a neighboring electronegative atom and interact strongly with it.

3) Covalent Bonding

Covalent bonding is a form of chemical bonding that is characterized by the sharing of a pair of a electrons between atoms or between atoms and other covalent bonds. Atoms can attain a more stable arrangement of electrons in their outermost shell by covalent bonds. Covalent bonds induce strong attraction at very short distances and are called strong bonds.

Summary of the interparticle forces is given in the flow diagram in Figure1.

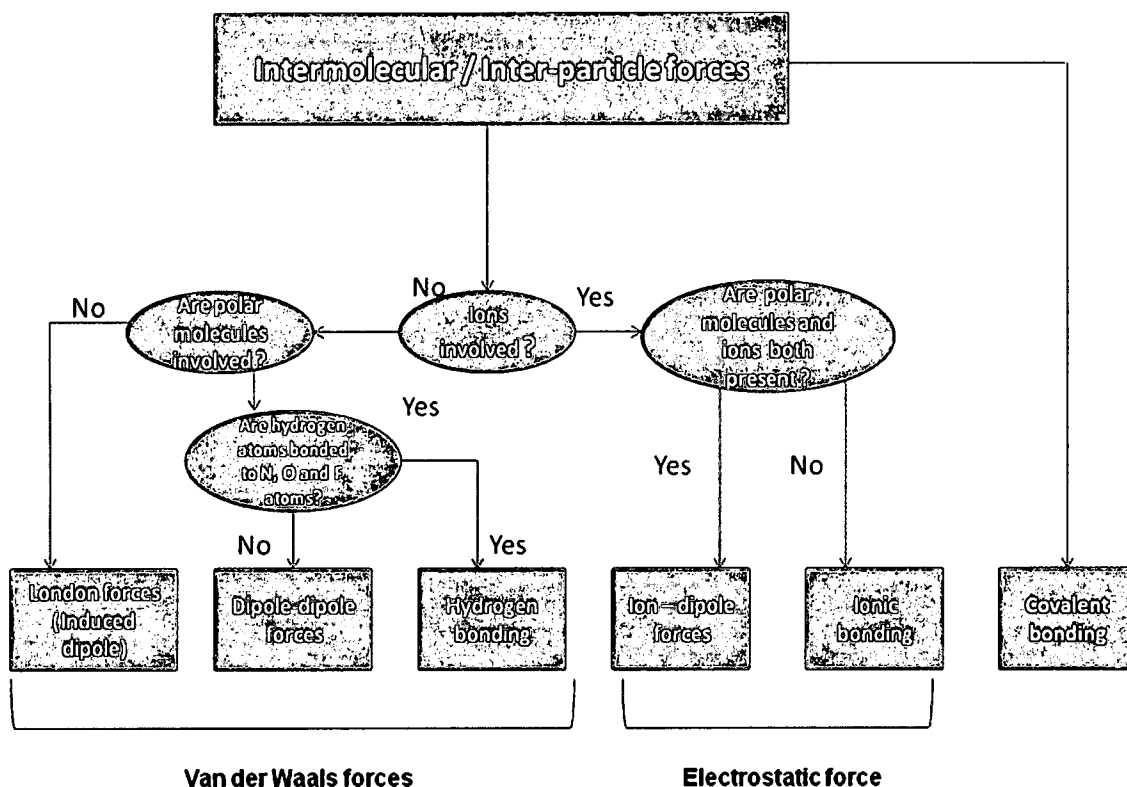


Figure 1: Flow diagram of intermolecular / interparticle forces

1.2.3) Interactive Forces of Powder Particles

The interactive forces of powder particles are van der Waals forces, electrostatic forces, and capillary forces.

i) van der Waals Force

This is a molecular interaction due to various polarization mechanisms. Because of their short interaction range, the overall magnitude of the van der Waals forces can be highly sensitive to the microscope surface structure. Thus, the effect of van der Waals forces can only be reduced but not completely eliminated. Though van der Waals forces are of electrostatic nature by fundamental mechanism, they are regarded as non-electrostatic forces when considering particle adhesion and cohesion. For particles without significant charge, van der Waals force would likely play a dominant role. The theoretical calculation for van der Waals forces between two spheres is given by,

$$F_{vdW} = AR/6h^2$$

Where A stands for Hamaker constant which is proportional to the surface energy of adhesion, $R = R_1 R_2 / (R_1 + R_2)$ is the reduced radius of the two interacting spheres of radii R_1 and R_2 and h is the minimum gap between the two spheres.

According to Lifshitz theory, the van der Waals force acting between two spherical particles with radius R at a separation distance $z \ll R$, can be given by

$$F_{vdW} = \frac{h\omega \cdot R}{8\pi z^2}$$

Where $h\omega$ is the Lifshitz- van der Waals constant which depends upon the material properties of the particles.

ii) Electrostatic Force

The electrostatic force F_e between two spherical particles is the short range attraction based on the columbic charge on the particle and the separation distance $z \ll R$, as shown in Figure 2. Krupp [14] has described the force:

$$F_e = \pi \epsilon_0 R \frac{U^2}{z} = \frac{q_1 q_2}{16 \pi \epsilon_0 [k_e + 1/2 \ln(2R/z)]^2 R z}$$

Where ϵ_0 is the permittivity of free space, U is the contact-potential differences between the particles, q_1 and q_2 are the charges on each particle and k_e is the Euler's constant of value 0.578. The charges can be attractive or repulsive depending on the signs of the interaction forces.

In electrostatic interactions that involve molecular polarization the force is directly proportional to the particle radius as given in the above equation. The dependence of the electrostatic force on radius was also given by Derjaguin approximation for interparticle forces [15]. The force between two spheres (Figure 2) in the z direction is given as

$$F_e = 2\pi \left(\frac{R_1 R_2}{R_1 + R_2} \right) W(D)$$

Where R_1 and R_2 are the radii of the two particles and $W(D)$ is the interaction free energy per unit area of two plane surfaces. For two equal spheres of radii $R = R_1 = R_2$, the equation reduces to:

$$F_e = \pi R W(D)$$

The interparticle force between a spherical particle and a flat surface is written as,

$$F_e = 2\pi R W(D) = 4\pi R \gamma$$

Where R is the radius of the spherical particle, γ is the surface energy of the flat surface and is conventionally defined as half the interaction energy, $W(D)$.

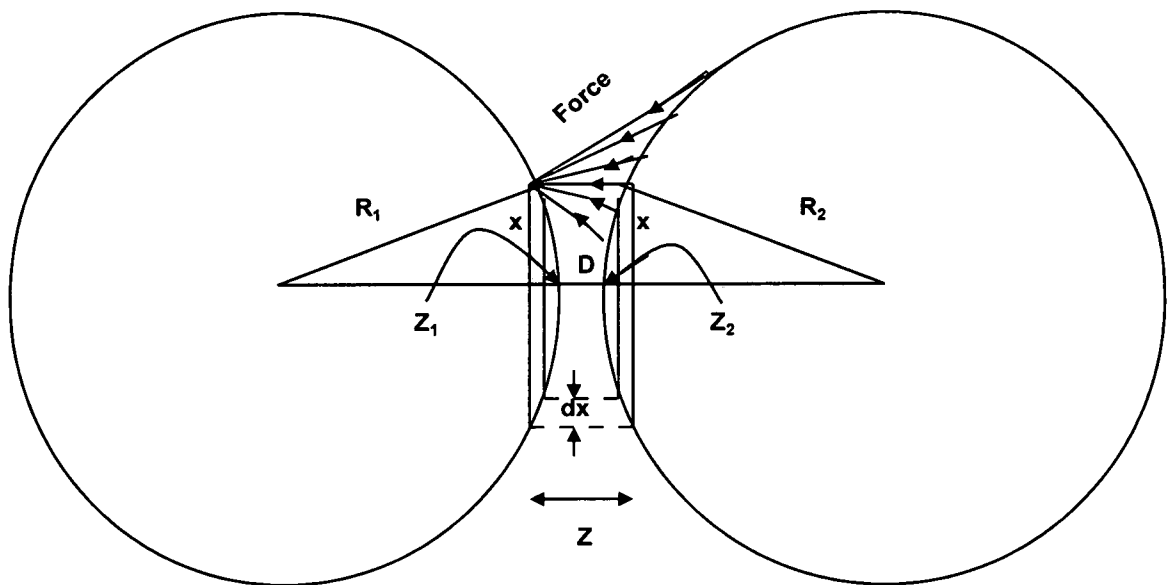


Figure 2: The Derjaguin approximation relating the force law F_e between two spheres of equal size (From [15])

ii) Capillary Forces

In powder particles, capillary force plays a significant role in the interparticle interaction. Water is spontaneously adsorbed from humidity in the air, and the moisture or the liquid bridge between two spherical particles could cause nano-sized powder particles to adhere to each other and increase the rate of clogging. The adhesive force between the spherical particles is given by the Derjaguin approximation as:

$$F_{\text{adhesion}} = 4\pi R\gamma_L \cos\theta$$

Where r is the radius of the spherical particle, γ_L is the surface tension of the liquid and θ is the contact angle between the spherical particle and liquid water.

1.3) Force Measurements

The simplest arrangement for measuring forces directly is the spring balance. The force was calculated using Hooke's law $F=kx$, where k is the spring constant, which is known and x is the displacement from the equilibrium position. In 1951, Derjaguin and Abrikossova performed the first accurate measurement of van der Waals force using force feedback technique, which was able to overcome the problem of spring instability. The development of a new instrument by Tabor and Winterton [16] in 1968 introduced important improvements in the measurement of surface forces. White light interferometry was employed [17] to detect the separation of the surfaces with much greater accuracy than had been previously possible. In the early 70's Tabor, Winterton, and Israelachvili

developed an instrument called surface force apparatus (SFA) [18] to measure surface-surface interactions. SFA has survived in various modified forms to become the instrument used in the majority of surface force measurements for the past 20 years. However the development of the atomic force microscope (AFM) in the late 80's enabled the measurement of surface forces with remarkable sensitivity, with force sensitivities of better than 10^{-10} N [19] being achieved.

1.4) Electrostatic Force Measurements

Depending on the method of measurement, electrostatic force techniques are known by a variety of names, including the atomic force microscope (AFM), the generic electrostatic force microscopy (EFM), scanning capacitance microscopy, Kelvin probe microscopy, scanning polarization force microscopy, and possibly others. Of all the techniques known, AFM is the most widely used instrument for measuring electrostatic forces between powder particles.

1.4.1) Atomic Force Microscope (AFM)

The development of the Atomic Force Microscope has produced a technique capable of measuring nano-Newton forces acting on a sharp tip as it approaches a substrate. The AFM is comprised of a flexible cantilever arm with a sharp tip. As the tip comes into close proximity to a surface, the arm will deflect due to interaction forces. The deflection experienced can be used as a feedback mechanism to map out features of the surface. This device has only been made

available with the development of nanometer-scale resolution provided by piezoelectric materials. Because of the operational range of the AFM, it makes an ideal instrument for studying these macroscopic interactions to determine the actual contribution due to these interaction forces. Ignoring any contributions due to capillary forces, the interactions between an AFM probe and sample are composed of two independent contributions. At long range (greater than a 10 nanometers), van der Waals and electrostatic forces are dominant. The AFM has already demonstrated versatility and flexibility with its range of operation. It has the capability of sub-nanometer resolution and sensitivity down to $\sim 10^{-12}$ N.

1.5) Significance of Atomic Force Microscope (AFM) in Force Studies:

The atomic force microscope (AFM) is not only a tool to image the topography of solid surfaces at high resolution. It can also be used to measure force-distance curves. Such curves, briefly called force curves, provide valuable information on local material properties such as elasticity, hardness, Hamaker constant, adhesion, and surface charge densities. For this reason, the measurement of force curves has become essential in different fields of research such as surface science, materials engineering, and biology. Another advantage of the AFM technique for force measurement includes the small area of interaction between probe and surface, minimizing problems with contamination. The significance of AFM is due to the nanometer-sized tip and the ability of the instrument to measure forces in the nano-Newton range. Forces that are measured in AFM include mechanical contact forces, van der Waals forces,

capillary forces, chemical bonding, electrostatic forces, magnetic forces, solvation forces , etc.

1.6) Background

NASA has continuously shown interest in developing lubricating coatings that can operate in the cold vacuum of space to very high temperature airframe bearings on the space shuttle and also to reduce dry sliding friction and wear in foil air bearings [20, 21, 22]. Solid lubricants have been developed in connection with these issues. The characteristics of solid lubricants validate their use when conventional lubricants are inadequate.

1. Thermal Stability: Good thermal stability ensures that the solid lubricant will not undergo any phase change or structural change at high or low temperature extremes.
2. Volatility: The lubricant should have low vapor pressure for the expected application at extreme temperature and low pressure conditions.
3. Chemical Reactivity: The lubricant should form a strong, adherent film on the base material.
4. Shear strength: The solid lubricant has low shear strength for friction reduction.
5. Compressive Strength: The solid lubricant has load supporting ability as it has high compressive strength.

NASA has been developing CaF_2 and eutectic $\text{BaF}_2 - \text{CaF}_2$ solid lubricant for many years and this type of coating is known as a composite solid lubricant

coatings because the solid lubricant is mixed with at least one separate phase of more wear – resistance matrix materials. So the solid lubricant is supplied with the matrix material to the sliding surfaces. BaF_2 - CaF_2 is a dielectric material that is highly resistant to the flow of an electric current.

NASA has developed various solid lubricants such as PS100, PS200, and PS300 for high temperature applications [23]. Though PS304 belongs to the family of solid lubricant coatings that was developed for the reduction of sliding friction and wear in turbomachinery systems, its importance of development was for improving finishing and performance characteristics. The composition of this coating is 60 wt% nichrome (80Ni-20Cr), 20 wt% chromia (Cr_2O_3), 10 wt% silver and 10 wt% eutectic barium fluoride-calcium fluoride (70BaF_2 - 30CaF_2). The constituents in powder form are deposited on the substrate by the plasma spray process. The powder feedstock for this coating was found to clog in the plasma spray system feed hopper. In a preliminary study, it was determined that eutectic BaF_2 – CaF_2 spherical particles (Figure 3) cling tenaciously to surfaces or to each other causing clogging in the plasma spray powder feeding system. When the BaF_2 - CaF_2 particles were smaller than 40 μm , the feedstock powder had poor flow characteristics. Therefore, in the case of PS304 coating the flow properties are dependent on the physical properties like the size of eutectic BaF_2 - CaF_2 particle, interparticle forces and environmental humidity.

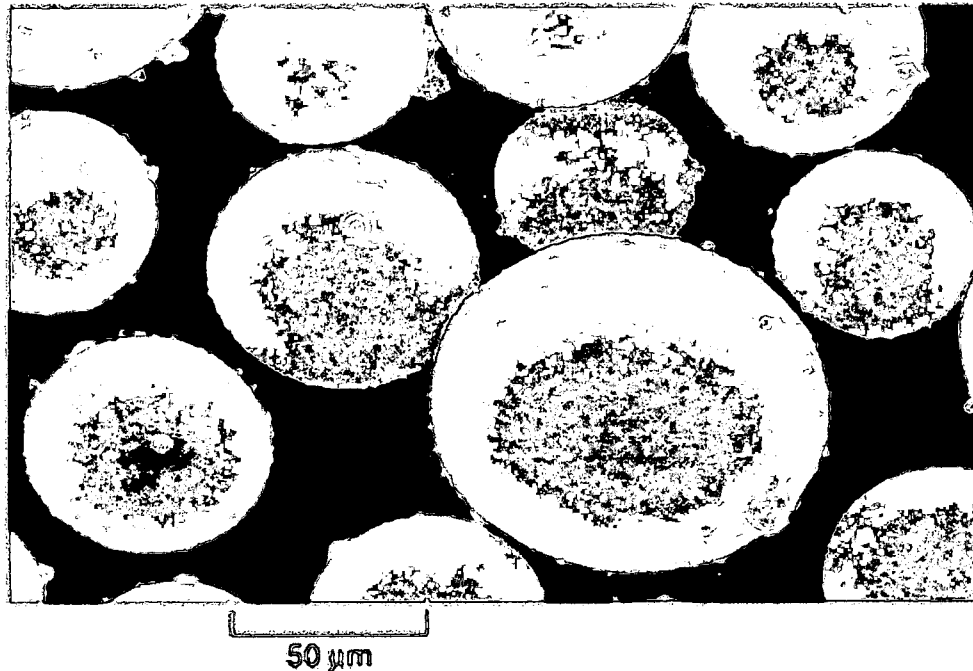


Figure 3: SEM images of spherical BaF₂ – CaF₂ particles

A recent investigation of the physical properties of the BaF₂-CaF₂ and PS304 feedstock by Stanford [22] reported that there were large quantities of sub-micron particles of comminuted BaF₂-CaF₂ from careful examination of Scanning Electron Microscope (SEM) images. The small particles tend to adhere to the larger particles by inter-particle friction, which influences the flow behavior of the powder system. Interparticle forces between the eutectic BaF₂-CaF₂ powder particles are affected by the presence of humidity and electrostatic charges. Due to this, there are large inter-particle forces experienced between the eutectic BaF₂- CaF₂ powder feedstock, which tends to create clogging during the production of solid lubricant coating. According to quantum mechanics, the electrons in materials can move spontaneously between discrete energy levels,

resulting in molecular polarization that causes attraction between neighboring surfaces at very small separation distances [9].

The existing literature on the flow properties of eutectic $\text{BaF}_2\text{-CaF}_2$ indicates that there is a need for understanding the role of inter-particle adhesive forces (humidity, electrostatic charges, van der Waals forces, etc.) to reduce the clogging in producing solid lubricant coatings. To address these issues, recently Tsai et al. [24] attempted to determine the role of humidity on adhesive forces using an AFM. Their results showed that at low humidity (<40%) the adhesion force is independent of the humidity and the particle diameter. A strong dependence on the particle diameter was observed in the high humidity region.

While Tsai et al.'s [24] experiments were first measurements in the direction of measuring inter-particle forces involving eutectic $\text{BaF}_2 - \text{CaF}_2$ particles, the substrate chosen was an ideal single crystal of CaF_2 and only the role of relative humidity was addressed. The present proposed research project addresses the role of electrostatic charges on interparticle forces between eutectic $\text{BaF}_2 - \text{CaF}_2$ particles. In this project, interparticle forces between a spherical particle probe of eutectic $\text{BaF}_2\text{-CaF}_2$ and a substrate of $\text{BaF}_2\text{-CaF}_2$ were obtained. This approach is quite close to the real situation in the feed stock used in plasma spray deposition of PS304 solid lubricant coatings. This configuration allows investigation of the role of electrostatic charges on the interparticle forces between eutectic $\text{BaF}_2 - \text{CaF}_2$ particles.

CHAPTER 2

INSTRUMENTATION AND EXPERIMENTAL METHOD

2.1) Introduction

Scanning Probe Microscope has been used for the measurement of forces between a spherical particle of eutectic $\text{BaF}_2\text{-CaF}_2$ and substrate of eutectic $\text{BaF}_2\text{-CaF}_2$. The Atomic Force Microscopy (AFM) belongs to a series of Scanning Probe Microscope invented by Binnig, Quate and Gerber in 1985.

A number of studies have been carried out using the surface force apparatus technique (SFA). However, the development of the AFM has provided another experimental option for the measurement of forces, especially the use of colloid probes, formed by attaching a single particle to the cantilever. Thus, the forces of known geometry are measured between surfaces in a way that facilitates theoretical analysis of the results.

2.2) Principle of AFM

The basic component and the working principle of an AFM are shown in Figure 4. The AFM consists of a cantilever with a sharp tip at its end that is used to scan the specimen surface. The cantilever is usually V-shaped to increase its lateral stiffness. Tips are typically made from Si_3N_4 or Si, and extended down from the end of a cantilever. When the tip attached to the cantilever is brought into proximity of a sample surface, forces between the tip and the sample lead to a deflection of the cantilever according to Hooke's law. A diode laser is focused onto the back of a reflective cantilever. As the tip scans the surface of the sample, moving up and down with the contour of the surface, the laser beam is deflected off the attached cantilever and it is measured by a position sensitive detector consisting of a dual element photodiode. A feedback loop then acts to move the piezo in the z direction taking the laser beam back to its original position. In this way, the sample is scanned with a constant force and the resulting piezo motion produces a topographical map of the region scanned with vertical resolution much smaller than 1 Å.

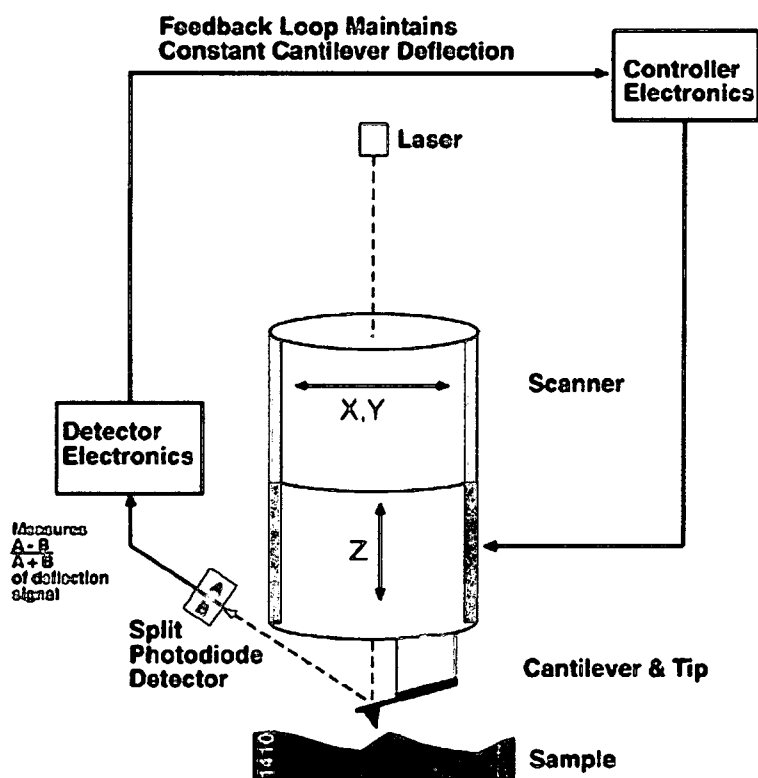


Figure 4: Schematic diagram of the working principle of an AFM (From [28])

2.3) Basic AFM Components

A generic AFM is comprised of the following components (Figure 5).

- Scanning system
- Probe tip
- Position sensitive detector
- Controller feedback electronics

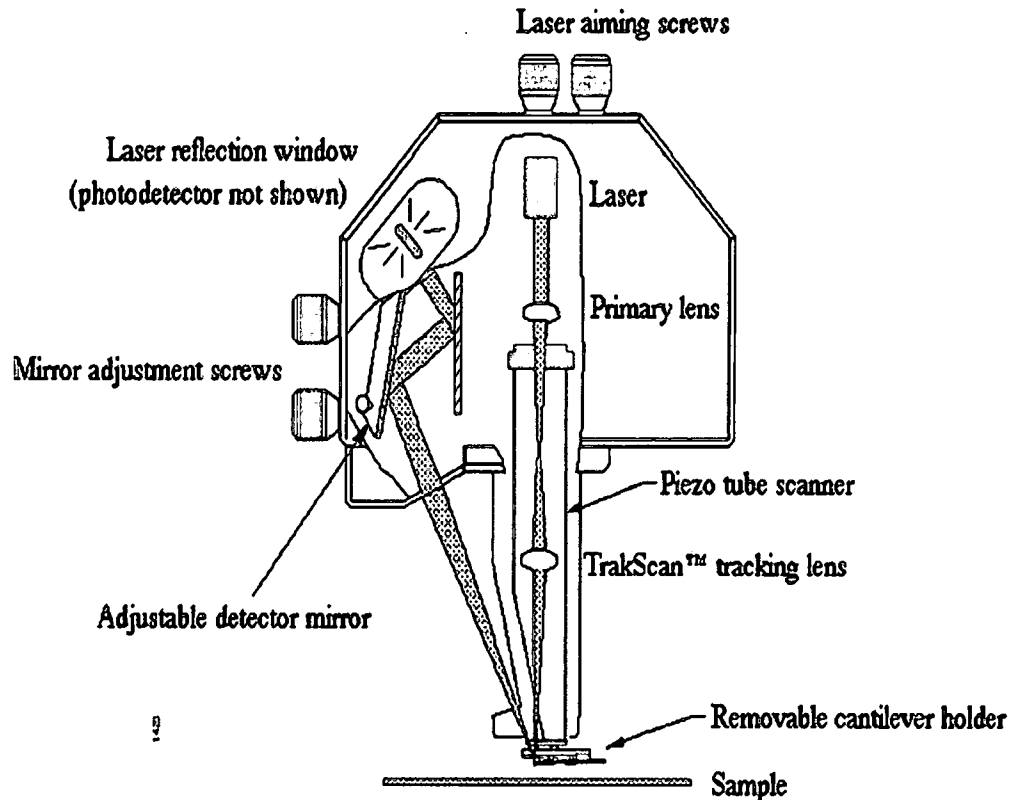


Figure 5: Basic AFM components (From [30])

Scanning System

The most fundamental component [25] of the AFM and the heart of the microscope is the scanner. The scanner is made from piezoelectric material which is typically used in order to provide sub-Angstrom motion control. In some models, the scanner tube moves the sample relative to the stationary tip and in

other models the sample is stationary while the scanner moves the tip. The piezoelectric tube scanner (Figure 6) expands and contracts proportionally to an applied voltage. All scanners have AC voltage ranges of +220 V to -220 V for each scan axis. The scanner is constructed by combining independently operated piezo electrodes X, Y, and Z into a single tube, forming a scanner, which can manipulate samples and probes with extreme precision in 3 dimensions.

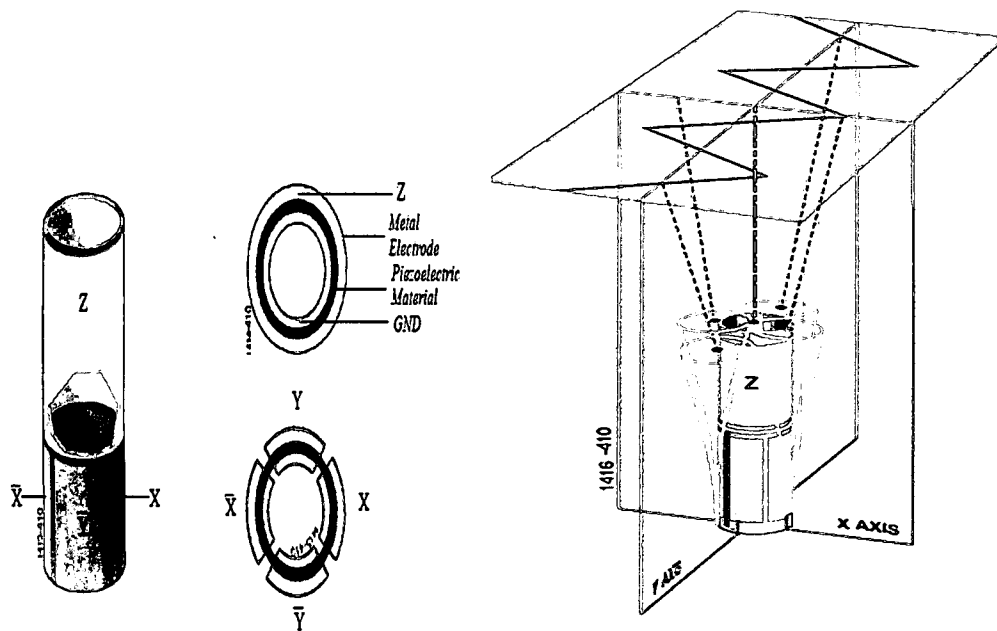


Figure 6: Piezoelectric scanner (From [28])

AFM Tips and Cantilevers

The AFM tip is mounted on a thin cantilever, which in fact is the key element of the AFM and its mechanical properties are largely responsible for its performance. Commercial cantilevers are typically made of silicon or silicon

nitride. The mechanical properties of cantilevers are characterized by the spring constant and the resonance frequency.

AFM tips are commercially micro-fabricated in three geometries, namely: (1) conical, (2) tetrahedral, and (3) pyramidal. Conical tips can be made sharp with a high aspect ratio (the ratio of tip length to tip diameter) making them especially useful for imaging features that are deep and narrow. Conical tips with diameters of 5 nm have been made, but they are easily broken. The pyramidal and tetrahedral tips have lower aspect ratios with tip diameters ranging 10 nm to 50 nm.

Cantilevers are usually fabricated as triangle or straight. The spring constant of the cantilever is strongly dependent on the physical dimensions: width, length and thickness and the elasticity of the material. The spring constant for triangle cantilever (Figure7) is expressed as follows:

$$k = \frac{Et^3w}{4l^3}$$

Where, k = spring constant
 E = Young's modulus
 t = thickness
 w = width
 l = length

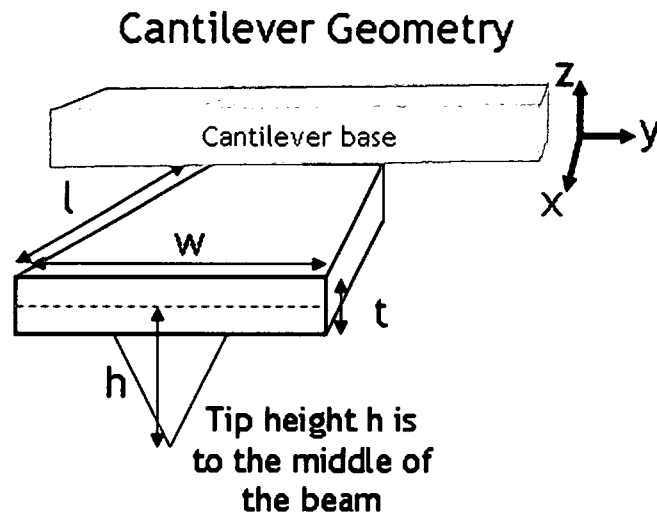


Figure 7: Triangle cantilever of the AFM (From <http://en.wikibooks.org/wiki/wiki/Nanotechnology/AFM>)

Colloidal Probe

In determining the interaction force between colloidal particles [26] the cantilever tip is modified by gluing the colloidal tip to the cantilever tip, which is generally referred as a colloidal probe. Different ways are used to attach microspheres to cantilevers. First, the colloidal spheres are glued to the cantilever. A long-chain linear polymer, often a thermoplastic, is used as glue. Solvents such as dichloromethane and dimethylsulfoxide are added as solvents to harden the glue. After solvents are evaporated completely the glued probe can be used for measurements. The glue can sometimes cause contamination, therefore spherical particles are sometimes melted or sintered onto the cantilever. Polymer particles are placed onto the end of the cantilever, and heated to close to the glass transition temperature. In this research work individual particles of eutectic $\text{BaF}_2 - \text{CaF}_2$ (Figure 8) are glued to the end of the cantilever tip.

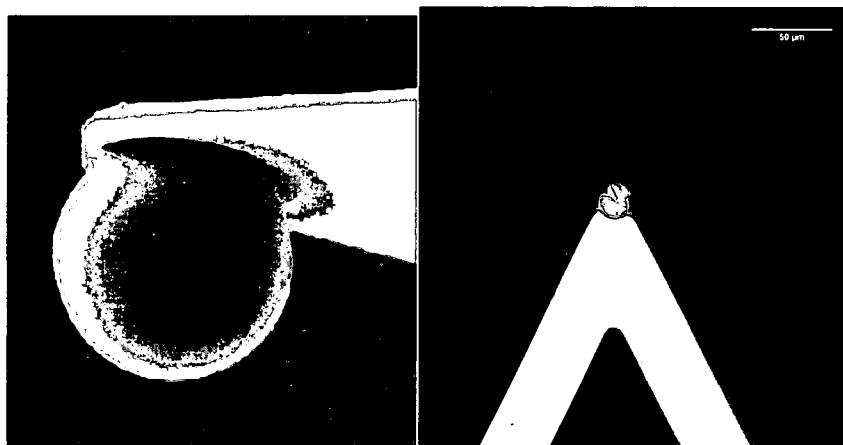


Figure 8: The spherical eutectic BaF_2 - CaF_2 particle attached to the tip of the cantilever

Beam Deflection Detection

The deflection of the cantilever is usually measured using the optical lever technique or beam deflection method (Figure 9). A beam of laser light from a solid state diode is reflected off the cantilever and collected by a position sensitive detector (PSD) consisting of two closely spaced photodiodes whose output signals are collected by a differential amplifier. Denoting the current from the top and bottom part of the photodiode as A and B, the signal used to measure deflection is $(A-B)/(A+B)$. At zero deflection the reflected laser beam is positioned in the center of the photodiode so that both segments show the same current and $A-B=0$. A deflection leads to a shift of the reflected laser spot and thus to a reduced signal on one segment and an increased signal on the other segment. With thermal noise limited, the beam deflection method can detect cantilever deflections less than 1 Å.

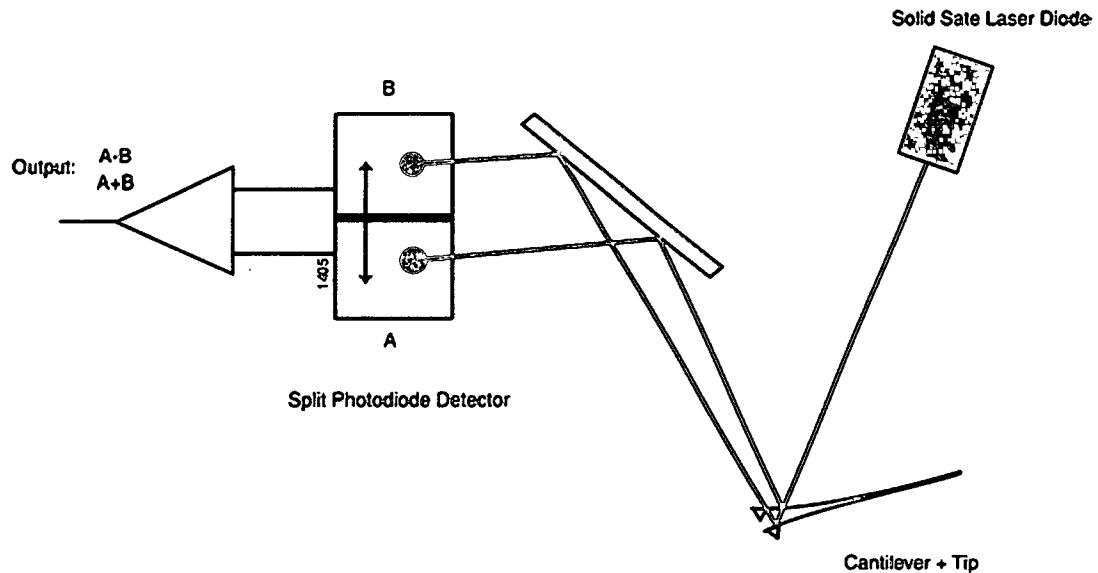


Figure 9: Beam deflection detection method (From <http://nue.clt.binghamton.edu/spm.html>)

Feedback Control

A feedback loop operates in two principle modes, such as with feedback control and without feedback control. With feedback control, a feedback loop maintains a constant deflection between the cantilever and the sample by vertically moving the scanner at each (x, y) data point to maintain the force at the pre-determined value. So by maintaining a constant cantilever deflection, the force between the tip and the sample remains constant. This mode of operation is said to be constant force mode or height mode where true topographical images are obtained. AFM is said to operate in constant height or deflection mode when the feedback control is turned off. There is always a small amount of feedback loop gain used to avoid thermal drift and the rough surface of the

sample damaging the tip. Operating without feedback control can also be called error signal mode.

2.4) Force Curve

The force curves are commonly used to set the imaging force in contact mode and to study attractive, repulsive, and adhesive interaction between the tip and the sample. A force curve [27] plots the deflection of the cantilever as it contacts and separates from the sample during the extension and retraction of the scanner. In the force calibration mode, the X and Y voltages applied to the piezo tube are held at zero and a saw tooth voltage is applied to the Z electrode of the piezo tube. On the force curve graph, the distance of the scanner movement is represented by the horizontal axis and the cantilever deflection by the vertical axis. The imaging of a force curve is shown schematically in Figure 10. When the tip of the cantilever comes towards the sample surface, the piezo extends (1) with no contact with the surface. In this region, if the cantilever feels long-range attractive force (or repulsive) force it will deflect downwards (or upwards) before making contact with the sample surface. As the tip approaches the sample, various attractive forces reach out and grab the tip (2). This region is called the jump-to-contact point and is usually due to electrostatic attraction or by capillary forces.

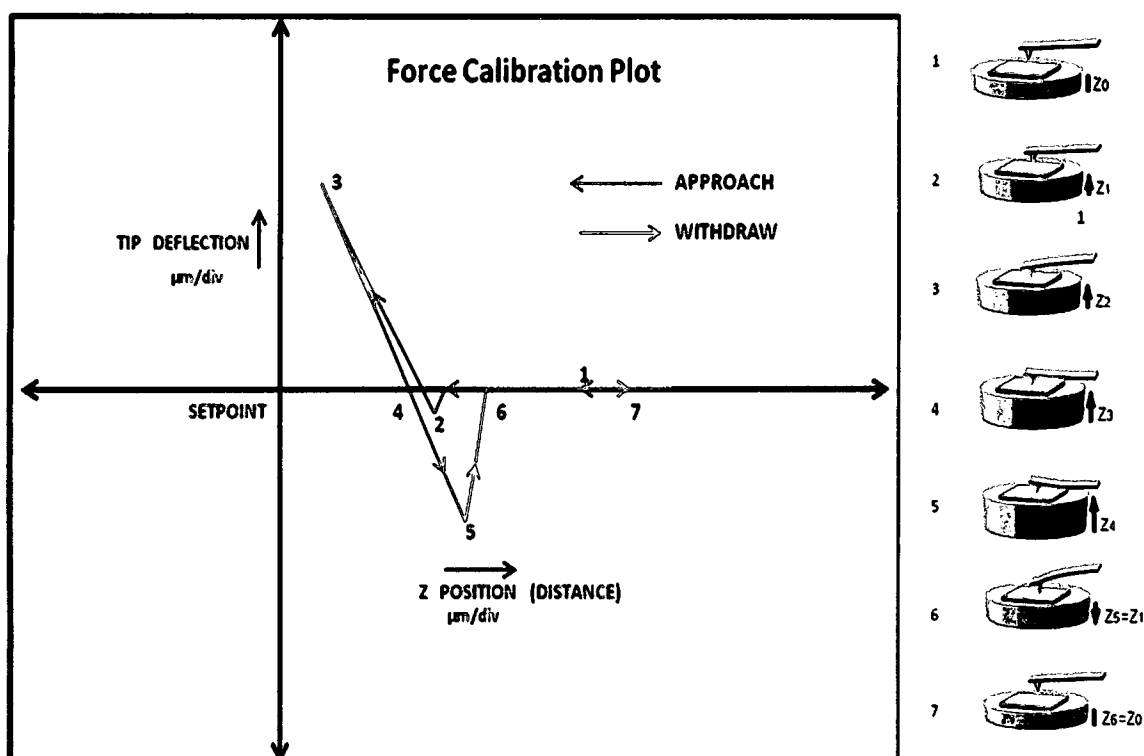


Figure 10: Typical force-distance curve (www3.physic.uni-greifswald.de/Method/afm/eafm.html)

Once the tip is in contact with the sample surface the cantilever bends upwards (3). As the tip presses into the surface, the piezo retracts and the cantilever relaxes downward until tip forces are in equilibrium with surface forces (4). The cantilever bends downward as surface attraction holds onto the tip (5) with the piezo continuing to retract. As the tip continues its ascent, it finally breaks free of surface attraction the cantilever is withdrawn and rebound upward (6). The region (7) represents that the cantilever is no longer in contact with the surface as the piezo continues to retract.

It is possible to extract information regarding the elasticity of the material by studying force curves. From the graph above, when the tip is in constant contact with the sample between points (2) and (3) with the tip pressed further and further into the material, the probe's cantilever flexes. The amount of cantilever flexion for a given amount of downward tip movement gives an indication of the material's elasticity. Use of force plots may also be used to adjust a setpoint, such that minimal force can be used during contact AFM which avoids sample damage and contamination.

2.5) Contact Mode

In contact mode, the probe or the tip is essentially dragged across the sample surface. In this mode, the tip is constantly adjusted to maintain a constant deflection, and therefore constant height above the surface. A bend in the cantilever corresponds to a displacement of the tip z relative to an undeflected cantilever and the force is calculated from Hooke's Law :

$$F = k \Delta Z$$

Where F = force

k = spring constant

ΔZ = cantilever deflection

Force constants usually range from 0.01 to 1.0 N/m, resulting in forces ranging from nN to μN in an ambient atmosphere. As the topography of the sample changes, the z-scanner moves the relative position of the tip with respect to the sample to maintain this constant deflection. Using this feedback mechanism, the

topography of the sample is thus mapped during scanning by assuming that the motion of the z-scanner directly corresponds to the sample topography. In constant force mode, the tip is constantly adjusted to maintain a constant deflection. Because the tip is in hard contact with the sample, the stiffness needs to be less than the effective spring constant holding atoms together which is about 10^{-10} N/m.

In contact mode [28], the attraction between the tip and the sample substrate increases until the electron clouds begin to repel each other electrostatically when the distance between them is decreased. This electrostatic repulsion weakens the attractive force and it reaches zero as the distance is further decreased. When the total van der Waals force become positive (repulsive), the atoms are in contact. This can be seen in Figure 11.

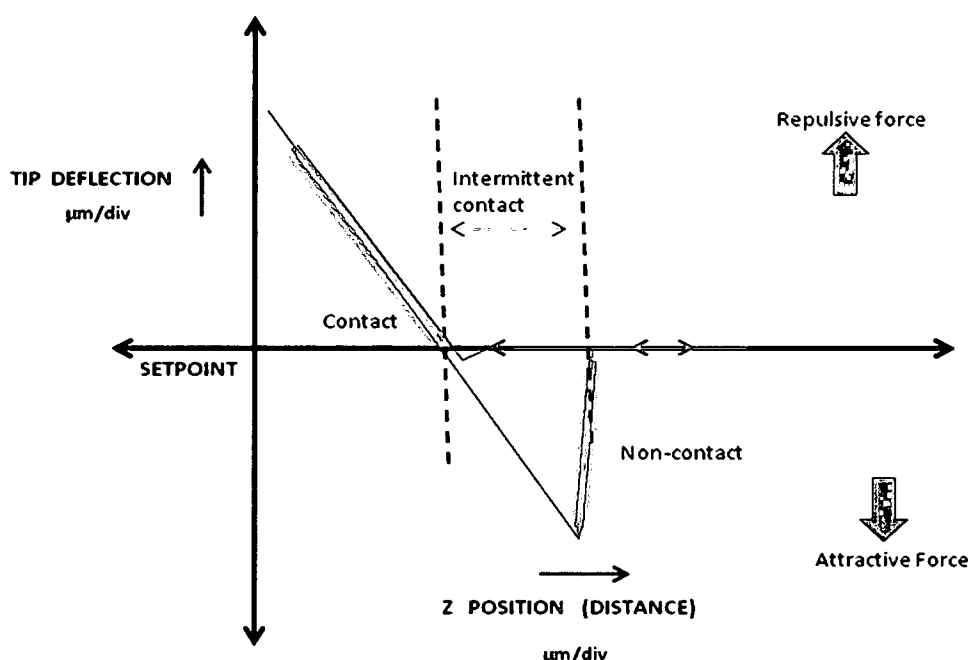


Figure 11: Force – distance curve

The van der Waals force is present in the repulsive or contact regime. The curve of van der Waals is steep in this region. As a result, the repulsive van der Waals force balances almost any force that attempts to push the atoms closer together. This is the reason why the cantilever bends when the cantilever pushes the tip against the sample rather than forcing the tip atoms closer to the sample atom. In addition to the repulsive van der Waals force, there are two other forces that are generally present in the contact mode of AFM: a capillary force exerted by the thin water layer on the sample substrate and the force exerted by the cantilever itself. The capillary force applies a strong attractive force that holds the tip in contact with the surface. The total force that the tip exerts on the sample is the sum of the capillary plus cantilever forces, and must be balanced by the repulsive van der Waals force for contact AFM.

2.6) Electrostatic Generator System

An electrostatic generator system produces static electricity or electricity at high voltage and low continuous current. The electrostatic generator system is excellently suited for temporarily bonding materials, adhesion between the material surfaces is brought about by generating an electrostatic charge. As a result, production processes can often be simplified and accelerated. An electrostatic generator system consists of a DC high voltage generator and one or several charging probes or electrodes. The probe consists of an inner bar of ionizing points mounted in a round rigid housing. The generator produces the high voltage points in the electrodes. The high voltage points produce ions to charge the materials, which then adhere to each other or to the other surfaces

electrostatically. The potential difference achieved has been used for a variety of practical applications such as operating X-ray tubes, sterilization of food, and nuclear physics experiments. The electrostatic generator has high efficiency in holding the electrostatic charge on the sample material for a sufficient time period. The generator system can operate in two different modes: constant current mode and constant voltage mode. In constant current mode, a charging current is set to a value and the system automatically adjusts the output voltage to maintain the set charging current value constant. In the constant voltage mode, voltage is set to particular value and the system maintains the selected voltage value constant regardless of the changes in the charging current values.

The electrostatic generator system PN57A (Figure 12) used in this study is a high voltage power unit adjustable between 0-30 kV at a maximum current of 5 mA. The high voltage points (Figure13) produce negative ions to charge the eutectic BaF_2 - CaF_2 substrate. Teflon is the inner bar with ionizing points that is surrounded by a glass fiber reinforced plastic which in turn is located within a rigid PVC housing. The electrodes are resistor protected to avoid spark over. The charging probe (Figure 14) consists of many high voltage points and it measures 1.3 x 0.8 inches with bar length of 25 inches. The material that has to be electrostatically charged has to be placed 10 mm – 20 mm from the charging probe for the produced ions to transfer to the material.

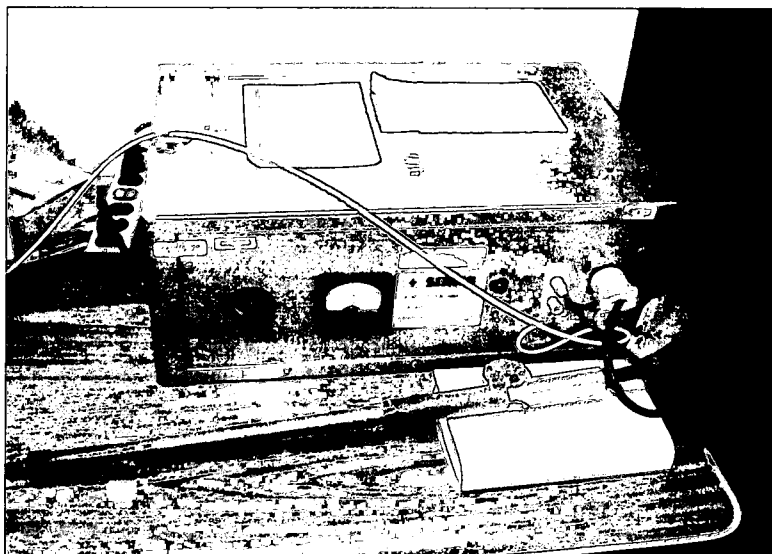


Figure 12: Electrostatic generator system PN57 with sample substrate

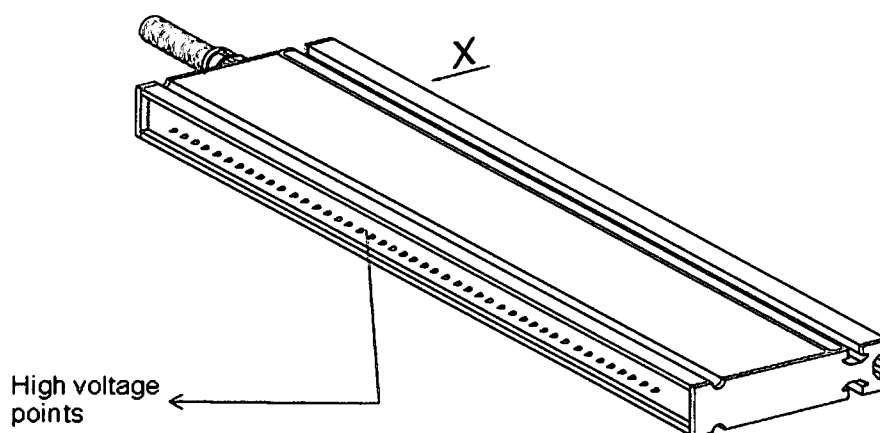


Figure 13: Typical charging electrode (From [www. Mksinst.com/docs/UR/ion-7430- Charging Bar DS.pdf](http://www.Mksinst.com/docs/UR/ion-7430-Charging%20Bar%20DS.pdf))

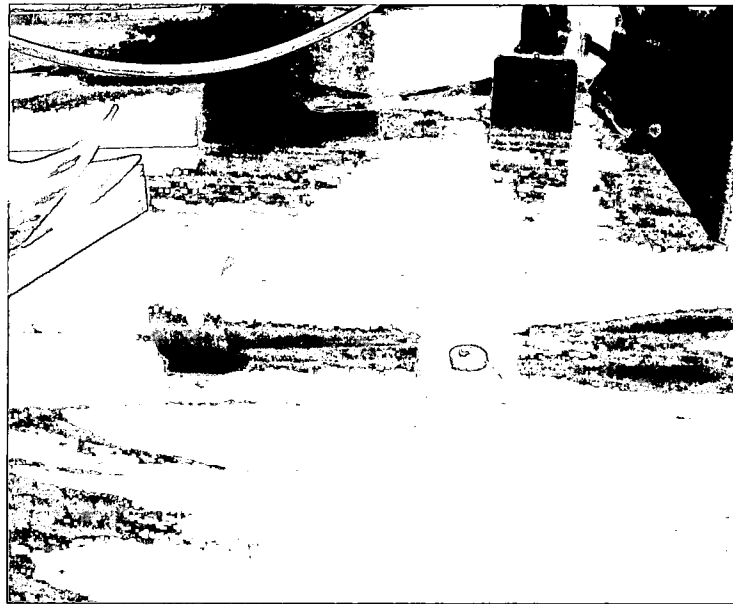


Figure 14: Probe or electrode of PN57A with sample substrate

2.7) Electrostatic Locator

Electrostatic locators measure the voltage, field and charge without transferring the charge to the instrument. They are used to determine if an electrostatic charge is present in a system, how much static electricity is present and the polarity of the charge. Simco SS-2X (Figure15) was used and this consists of a meter that senses the presence of charge on the surface of the sample object. An electrostatic locator meter is also known as an electrostatic field meter, which measures the electrostatic field produced by the charged surface by using a reference sensor. This sensor must be referenced to ground and the distance between the locator and the sample object should be well known for accurate measurements. This locator ranges from 0-200,000 V and 0 – 4000 kV/meter.

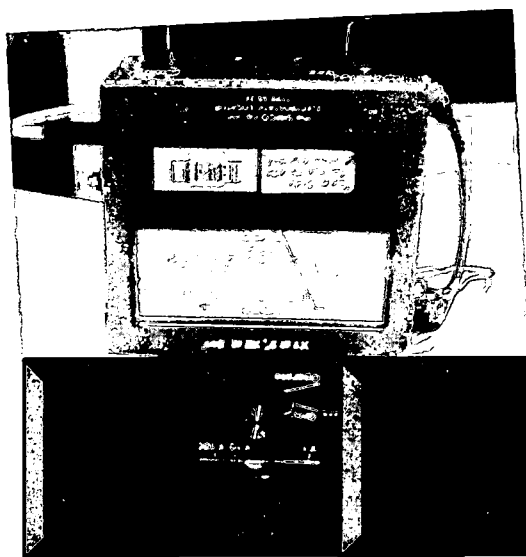


Figure 15: Electrostatic locator SIMCO SS-2X

2.8) Experiment

A Digital- Instrument Dimension 3000 scanning probe microscope [29] was used for the measurement of force between a particle probe of eutectic BaF_2 - CaF_2 and a substrate of BaF_2 - CaF_2 . The basic principle of interactive force measurement using AFM is to bring the tip cantilever into contact with the substrate and to record the displacement of the tip-cantilever as it detaches and follow the z-piezo displacement [Force-Distance Curve analysis]. The inter-particle forces act on the tip from the time it is in contact with the substrate until it finally detaches from the substrate. The interactive force prior to detachment will be stronger than the resilient force of the cantilever. After that, the cantilever resilient force will be stronger than the interactive force and therefore the tip detaches from the surface. Thus, at the moment the tip loses contact with the substrate, the interactive force will be equal to the resilient force of the cantilever.

The inter-particle force is determined with the knowledge of the spring constant and deflection of the cantilever using Hooke's law. Powder particles of eutectic BaF_2 - CaF_2 ($5\mu\text{m}$ - $50\mu\text{m}$) were manufactured by gas atomization which are used for both substrate and AFM cantilever tips. The substrate of eutectic BaF_2 - CaF_2 was obtained by compaction of the powder particles at high pressure. Individual particles of different diameter ($21\mu\text{m}$ – $30\mu\text{m}$) isolated from the eutectic BaF_2 - CaF_2 powder were used to replace standard AFM tips with known spring constants. AFM was used to measure the electrostatic force between the eutectic BaF_2 - CaF_2 particle and the eutectic BaF_2 - CaF_2 substrate by analyzing the force displacement curves obtained at various locations on the substrate.

A Scanning Electron Microscope (SEM) was used to generate electrostatic charges on the eutectic BaF_2 - CaF_2 substrate in the first phase as used earlier by Z. Hongben, G. Martin and P. Wolfgang [30]. Charging at different potentials for a fixed time or fixed potential for varying times were used for obtaining controlled amount of electrostatic charges on the substrate. Immediately after exposing the substrate in SEM, it was carefully transferred to the AFM for electrostatic force measurements. But this method was not effective as the electrostatic charge on the sample substrate dissipated very fast before the force-displacement curve could be obtained.

Since the SEM charging was not effective, a static generator PN57A described in detail previously was used to generate electrostatic charges on the sample substrate. A constant voltage mode of operation was performed and the sample substrate was charged with a negative potential of 10 kV for 10 minutes

to obtain a controlled amount of electrostatic charge on the substrate. The changing current value was from 0.5 – 1 mA. The amount of charge retained on the sample after a significant time period of charging was also recorded using electrostatic locator. A distance of 2.5-5 inches was maintained between the locator and the substrate to obtain accurate measurements. Precautions were taken in handling the charged substrate so that the electrostatic charge would not get dissipated before obtaining the AFM measurements. It was found that the electrostatic charge generated on the eutectic $\text{BaF}_2\text{-CaF}_2$ substrate was retained for 6 minutes. Force measurements were taken at several locations on the substrate to determine the spatial variability. Measurements as a function of the amount of electrostatic charge were compared with measurements performed without charging. The inter-particle force measurements between the eutectic $\text{BaF}_2\text{-CaF}_2$ and substrate of eutectic $\text{BaF}_2\text{-CaF}_2$ were then examined theoretically following the Derjaguin approximation.

CHAPTER 3

RESULTS AND DISCUSSIONS

3.1) Introduction

This section gives an overview of the results of the force curve obtained showing the effect of electrostatic charge between the particle probe of eutectic BaF_2 - CaF_2 and a substrate of BaF_2 - CaF_2 . For obtaining this effect, a charge – time relation called the master curve was established. This master curve was used in the analysis of the electrostatic force to convert the time factor to charge. The time dependence of the electrostatic force on the force curve for fixed location and with different diameter tip was determined. The effect of electrostatic charge on the force curve at various locations on the substrate surface was also determined. All the force curves were obtained by electrostatically charging the substrate with a negative potential of 10 kV and for 10 minutes.

3.2) Charge –Time Relation of Eutectic BaF₂-CaF₂ Substrate

The eutectic BaF₂-CaF₂ substrate was electrostatically charged with the static generator and the charge retained on the substrate was recorded. After 10 minutes of charging, the charge retained on the sample was recorded with the electrostatic locator every 10-20 seconds. Five sets of readings were obtained at room temperature for the above mentioned potential and time. The average value of charge remaining on the substrate was calculated and an exponential curve was plotted as a function of time as shown in Figure 16.

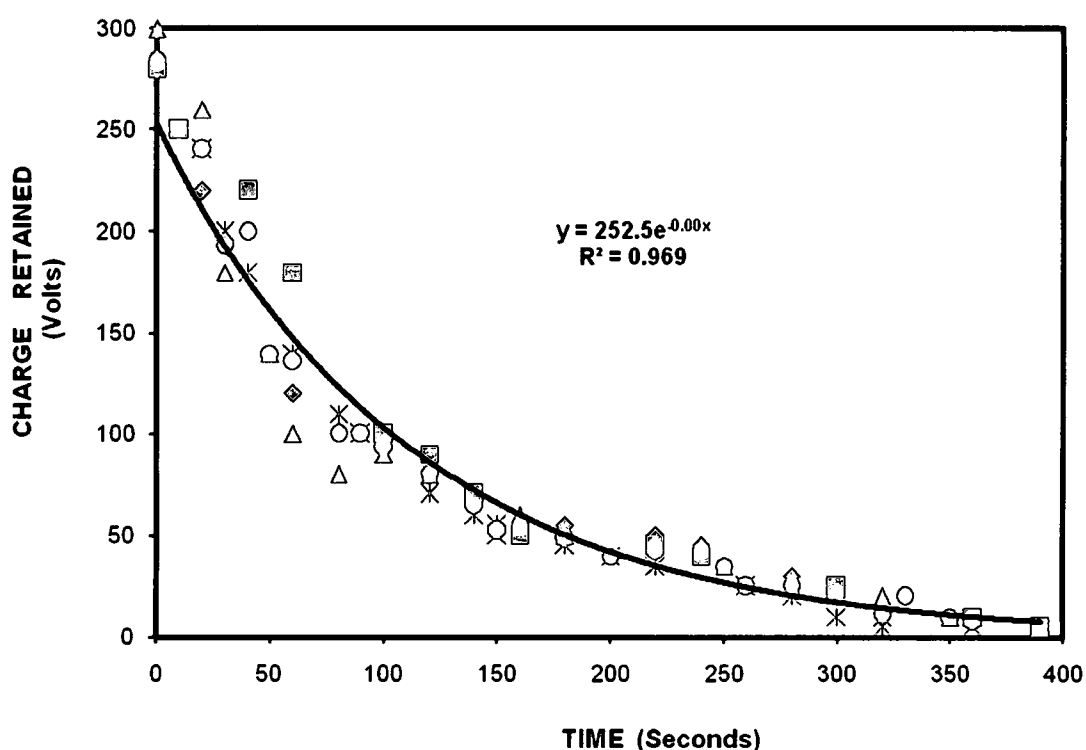


Figure 16: The dissipation of substrate electrostatic charge with time

It was observed that there was a gradual decay of charge from the substrate with increasing time. After 400 seconds, the charge on the substrate completely decays. Therefore, it is evident that there could be charge remaining on the substrate due to electrostatic effect for approximately 6 minutes at least. This relation between time and charge provides the approximate charge that could be remaining on the substrate when the force –distance curves are obtained by the AFM. It took approximately 90-120 seconds to transfer the charged substrate from the electrostatic generator to the AFM and to engage the AFM for obtaining the force-distance curve. After 120 seconds, the charge on the substrate dissipated and came down to 90 volts. In considering other limiting factors such as the environmental condition and the distance between the sample substrate and the charge locator, the charge remaining on the sample substrate will vary more than the charge that is shown in the master curve graph. Therefore, the charge remaining on the substrate was approximately 70 volts when the AFM was engaged for obtaining the force – distance curve. The electrostatic force is directly proportional to the charge on the substrate. The higher the charge retained on the sample, the higher the electrostatic force will be. All the force curves were obtained within the time range of 120 – 400 seconds.

3.3) Effect of Electrostatic Charge on the Force Curve

The measurement of electrostatic force by AFM between the particle probe of eutectic $\text{BaF}_2\text{-CaF}_2$ and a substrate of $\text{BaF}_2\text{-CaF}_2$ was obtained by Force –Distance analysis. The force curves for an uncharged substrate and for a charged substrate were compared. Figure 17 shows the force-distance curve for the uncharged substrate of $\text{BaF}_2\text{-CaF}_2$. Figure 18 shows the force-distance curve for electrostatically charged substrate of $\text{BaF}_2\text{-CaF}_2$. The electrostatic charge on the substrate of eutectic $\text{BaF}_2\text{-CaF}_2$ causes the cantilever to deflect as it approaches the sample but is not yet in contact with the substrate. The distinctive deflection in the plot was due to electrostatic charge, which is a long range attractive force and the force was calculated by Hooke's law.

In Figure 19, it can be seen that there is deflection in the cantilever in the upward direction because of long-range attractive force. The attractive force experienced by the cantilever was because of electrostatic charge that was retained on the substrate. Electrostatic force is usually strong over long range. Therefore, the measurement of the downward deflection of the cantilever will give the exact electrostatic interaction between the tip and the substrate. The repulsive van der Waals force is significant in the contact regime. With the intermittent contact of the probe and the substrate, both van der Waals and electrostatic force interactions were observed.

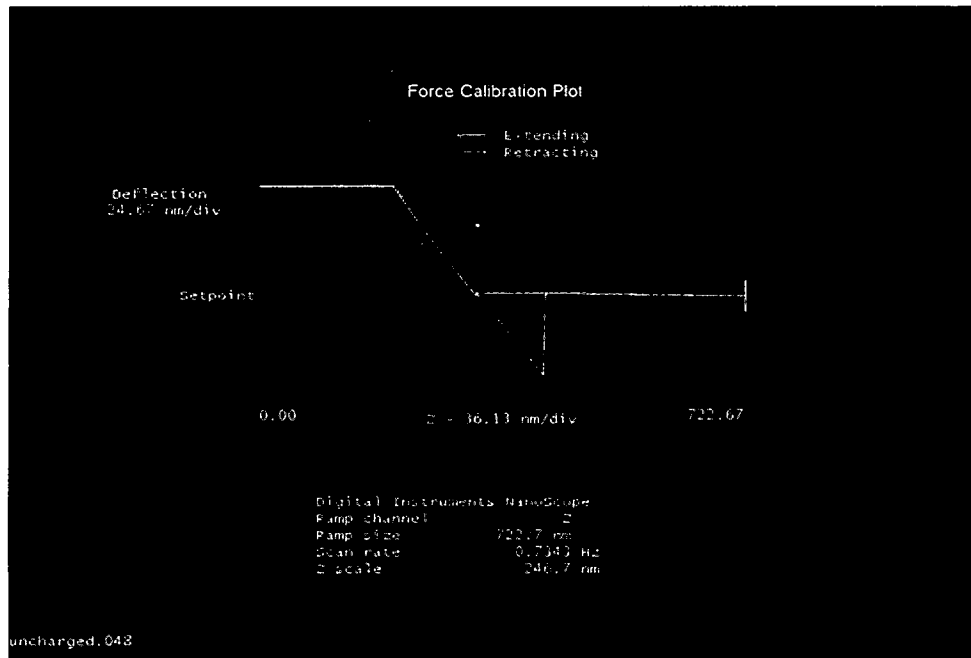


Figure17: The force –distance curve of **uncharged** eutectic $\text{BaF}_2\text{-CaF}_2$ substrate

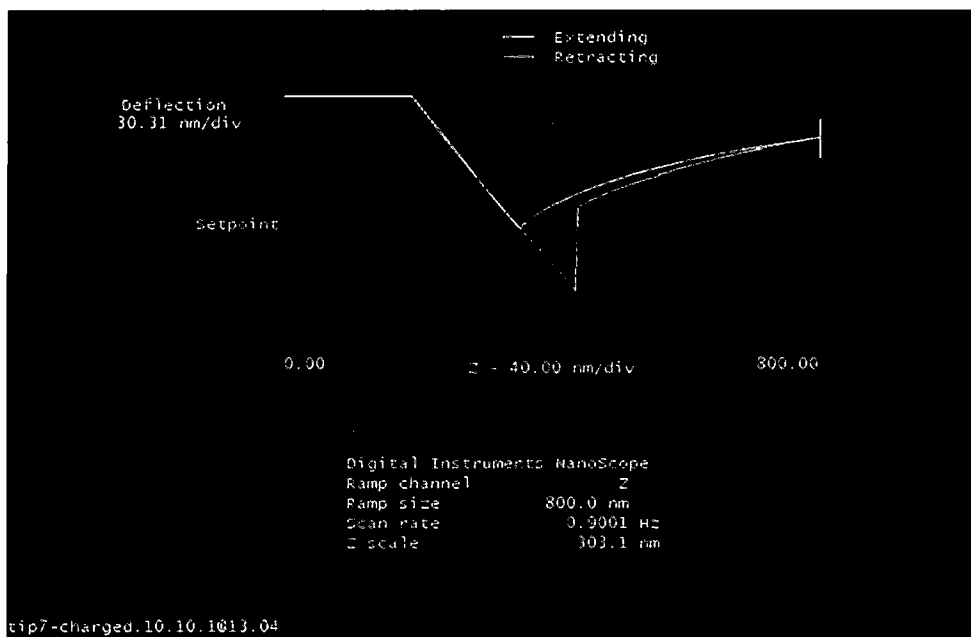


Figure 18: The force –distance curve of **charged** eutectic $\text{BaF}_2\text{-CaF}_2$ substrate

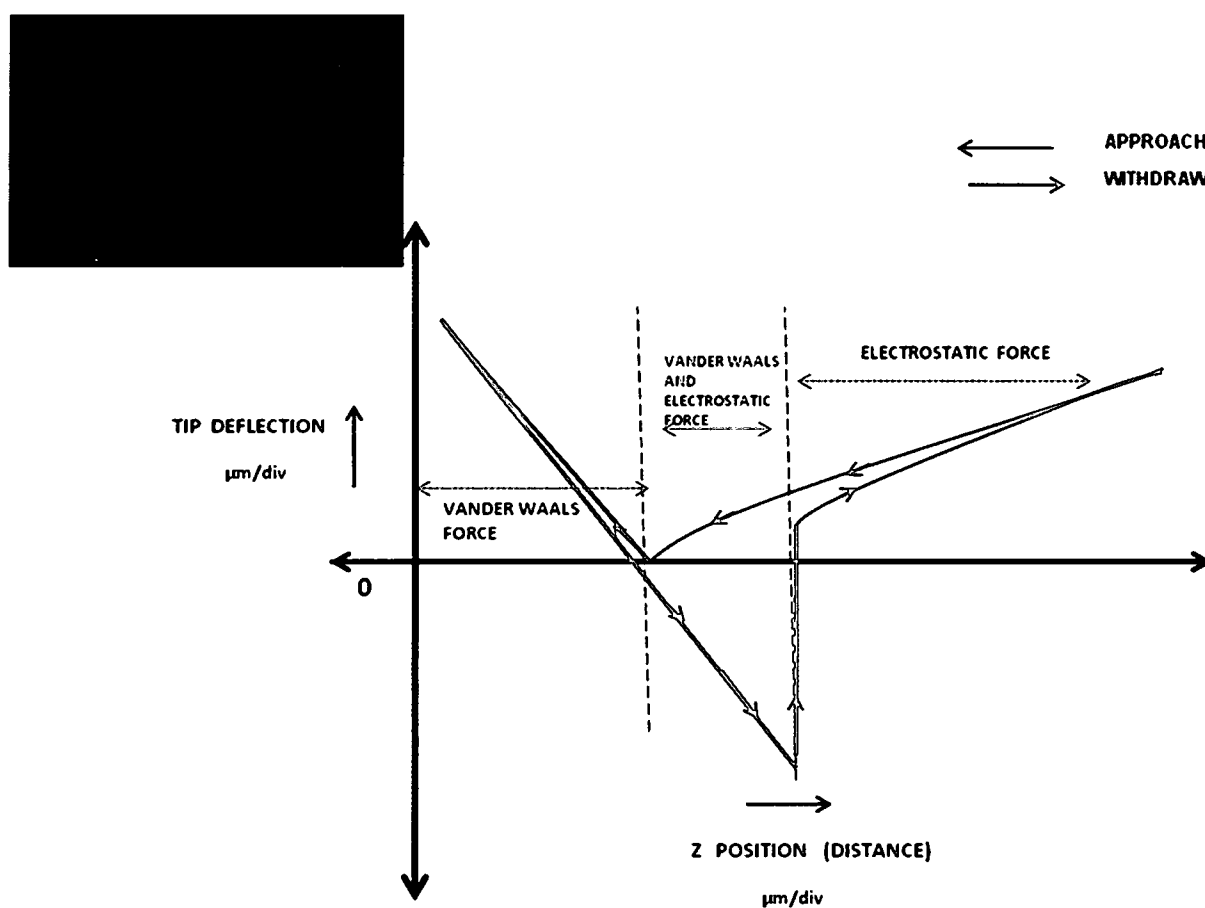


Figure 19: Electrostatic and van der Waals forces

The difference in force for uncharged and charged eutectic $\text{BaF}_2\text{-CaF}_2$ substrate was calculated with different diameter tips to determine the variability of electrostatic charge on the force-distance curve. The difference in force gives the electrostatic force between the tip and the substrate. The force difference was calculated for z position of the cantilever from long range to short range. As the electrostatic force is strong over a long range, larger electrostatic force was observed when there was more distance between the cantilever and the

substrate. The distance was taken as the z distance moved by the piezoelectric scanner.

The above calculated electrostatic force can be related to the "Columbic Law". Figure 20 shows the plot between force and inverse square of the distance between the probe tip and the substrate.

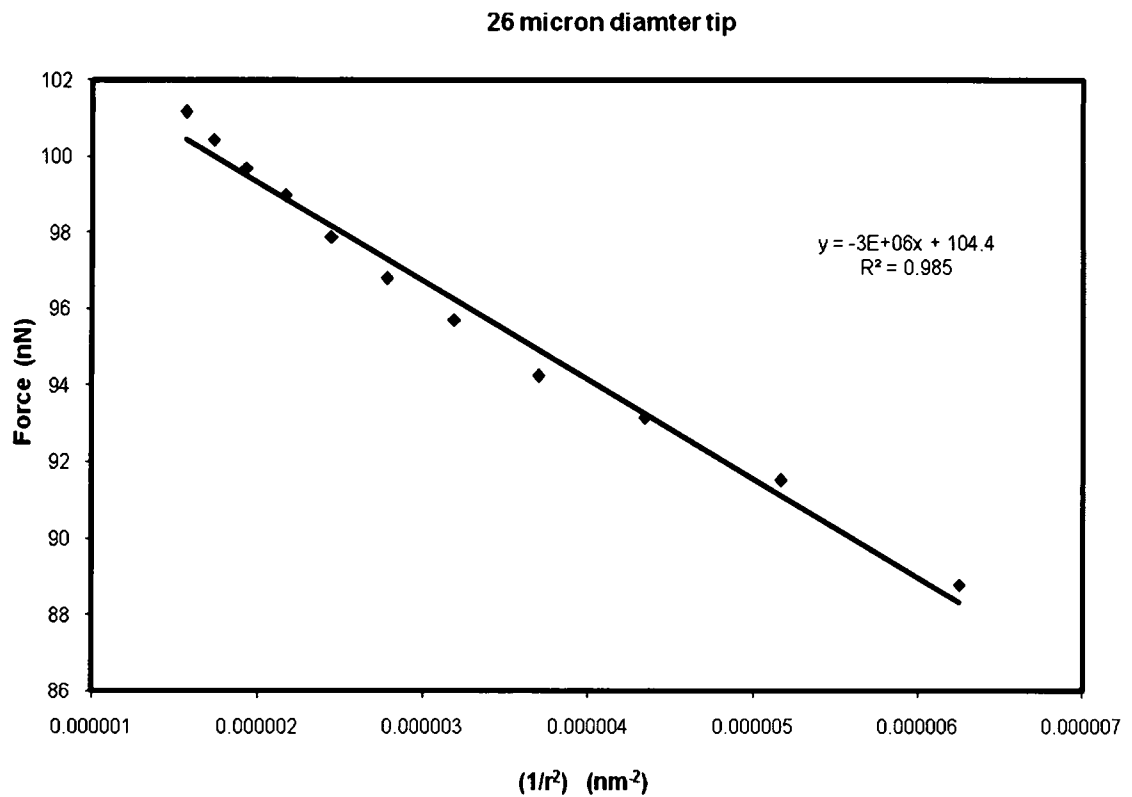
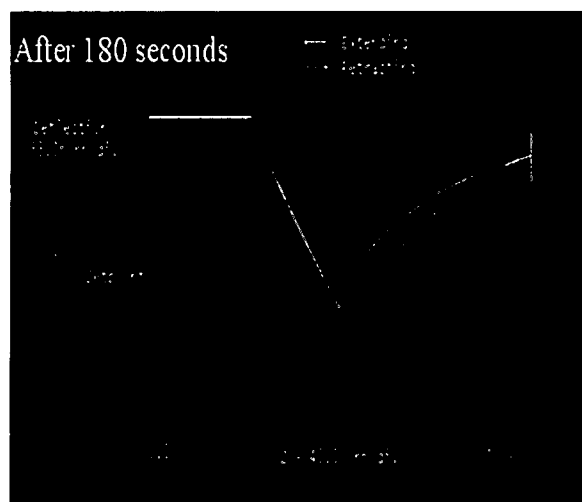


Figure 20: Force as a function of distance

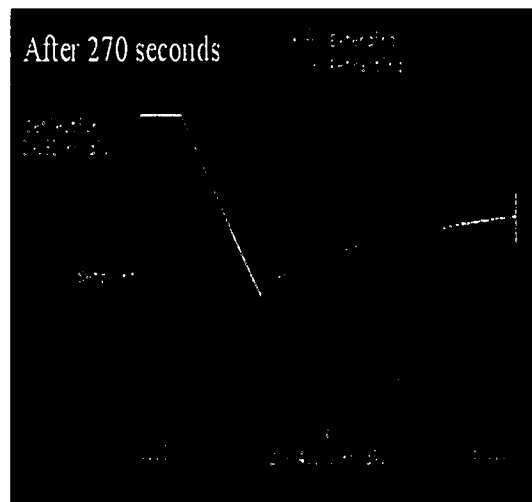
3.4) Time Dependence of Electrostatic Charge on the Force-Distance Curve

In Figure 21, the force-distance curves show the dissipation of electrostatic charge for charged substrate of eutectic $\text{BaF}_2\text{-CaF}_2$ with respect to time. The initial charge retained on the substrate was approximately 70 volts and the force-distance curve for dissipation of charge with respect to time was recorded. As charge on the substrate decays with time, the electrostatic force should decrease with respect to time. This was observed from the force-distance curve as a function of time. The force distance curve was analyzed and it was observed that the deflection of the cantilever decreased with increase in time. When the attractive force due to electrostatic charge completely decays, the electrostatic force becomes zero.

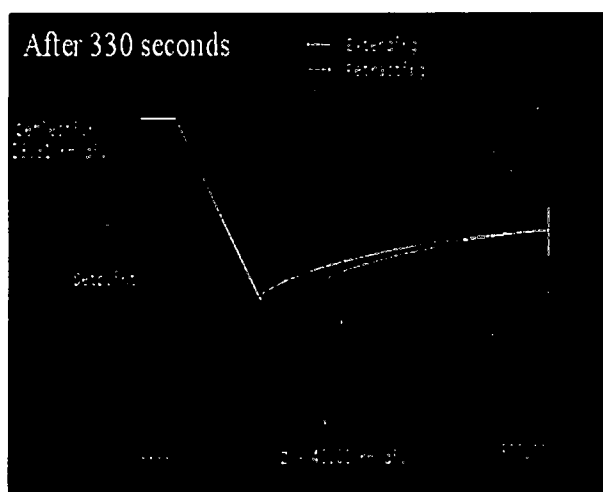
Figure 21(a) was obtained after 180 seconds, which shows that there was enough charge retained on the sample with substantial deflection observed. The curvature changed and the bending in the force curve reduced with increase in time. Figures 21(b) and (c) were obtained after 270 seconds and 300 seconds, respectively. Figure 21(d) shows that there remains almost no charge on the substrate after 400 seconds, with minimal deflection of the cantilever.



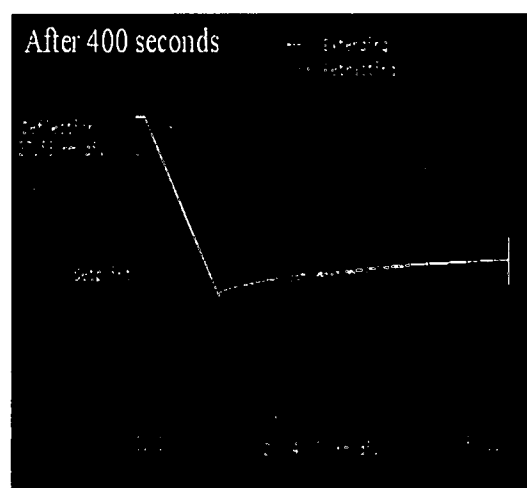
(a)



(b)



(c)



(d)

Figure 21: Time dependence of electrostatic charge on the force-distance curve

3.5) Effect of Electrostatic Charge on the Force Curve as a Function of Tip Diameter.

Three varying factors were involved in the measurement of the electrostatic force. They are (1) the location on the sample substrate of eutectic $\text{BaF}_2\text{-CaF}_2$ where the cantilever tip of eutectic $\text{BaF}_2\text{-CaF}_2$ comes in contact. (2) the time at which the force – distance curve was measured. (3) the charge retained on the substrate when the force curve was obtained. As has been discussed, the time and charge were dependent on one another. This can be seen from the charge dissipation chart in Figure 16. The force – distance curve obtained at various times highly influenced the force calculation.

As the substrate of eutectic $\text{BaF}_2\text{-CaF}_2$ was obtained by compaction of the powder particles at high pressure, the surface of the substrate was rough. The roughness, protrusions in the spherical particles and the particle size distribution, highly influenced the force curve. So the force curve measurement was possible only at certain locations on the substrate. The limitation such as roughness, protrusions in the spherical particle of eutectic $\text{BaF}_2\text{-CaF}_2$ and the particle size distribution are discussed in detail in the following section. Getting a good force-distance curve at the right location within the time range of 5-6 minutes before the charge could decay from the substrate of eutectic $\text{BaF}_2\text{-CaF}_2$ was challenging.

In the first step, the force-distance curve was obtained at a fixed location on the substrate with the dissipation of the electrostatic charge with time. A position on the substrate of eutectic $\text{BaF}_2\text{-CaF}_2$ was selected and a skillful

marking was done on the substrate surface with a marker to have the force-distance curve at that particular location. In this way, it was easy to locate the position on the sample substrate when engaging the cantilever tip of eutectic $\text{BaF}_2\text{-CaF}_2$. The substrate of eutectic $\text{BaF}_2\text{-CaF}_2$ was electrostatically charged and was carefully transferred to the AFM. The cantilever tip was brought in contact with the selected location and the force-distance curve was recorded. The deflection of the cantilever for 24 μm and 26 μm diameter tips was compared (Figure 22).

After 240 seconds, the deflection, or the curvature, in the force curve for the 26 μm diameter tip was more than that of the 24 μm diameter tip. From the master curve, there remains very little electrostatic charge on the substrate after 360 seconds. For 24 μm there was complete decay of charge after 420 seconds, but for 26 μm diameter tip, deflection of the cantilever does not come to the setpoint value even after 420 seconds which indicates that there still remains some electrostatic charge on the substrate. So a strong dependence of particle diameter was observed in the measurement of electrostatic force.

24 micron diameter tip

26 micron diameter tip

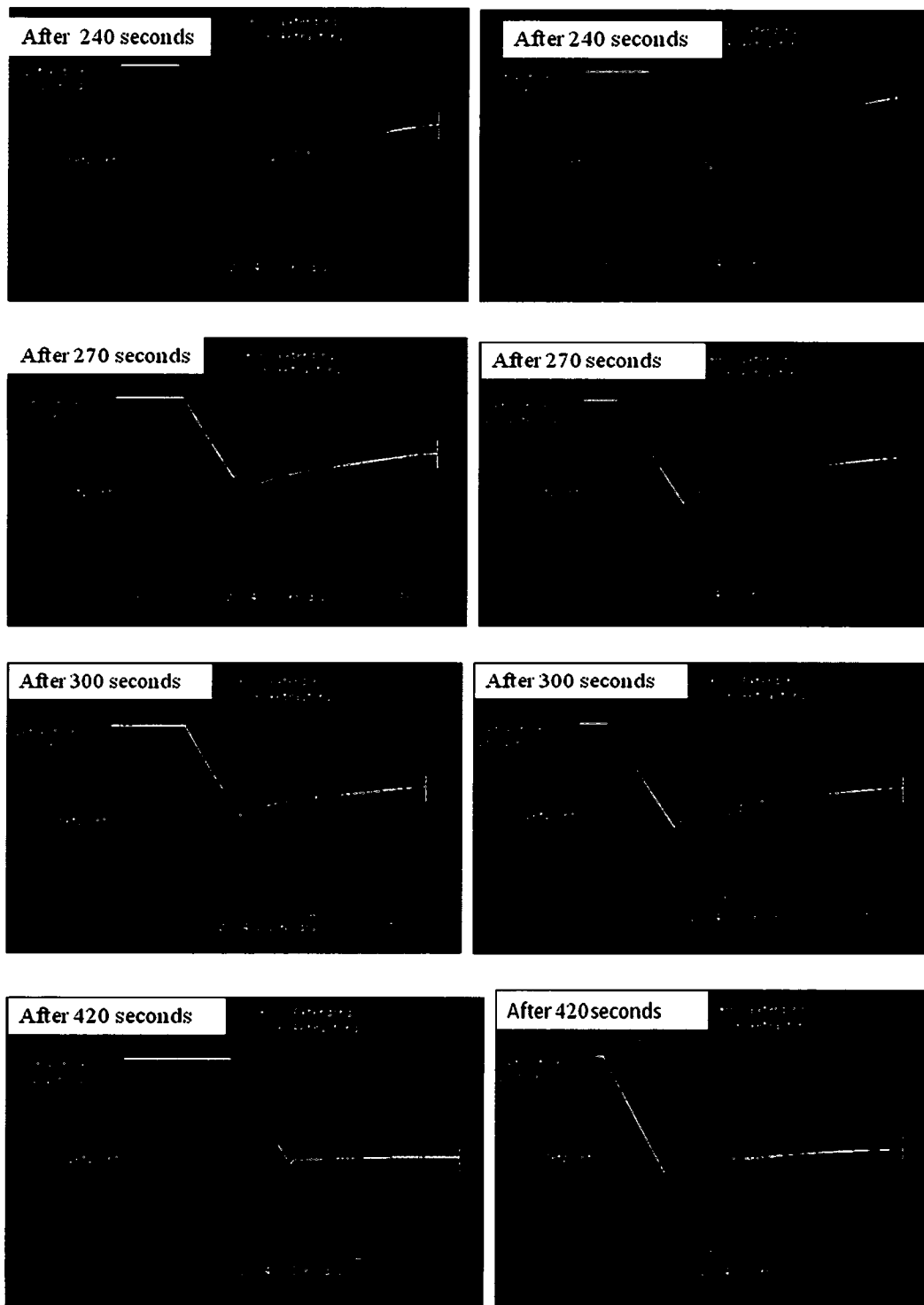


Figure 22: Time dependence of electrostatic charge on the force-distance curve for different tips

With the force curve obtained for different diameter tips, the total force was calculated by Hooke's law and a graph was plotted relating total force and time (Figure 23). An exponential curve was fitted which shows a decrease in force as a function of time.

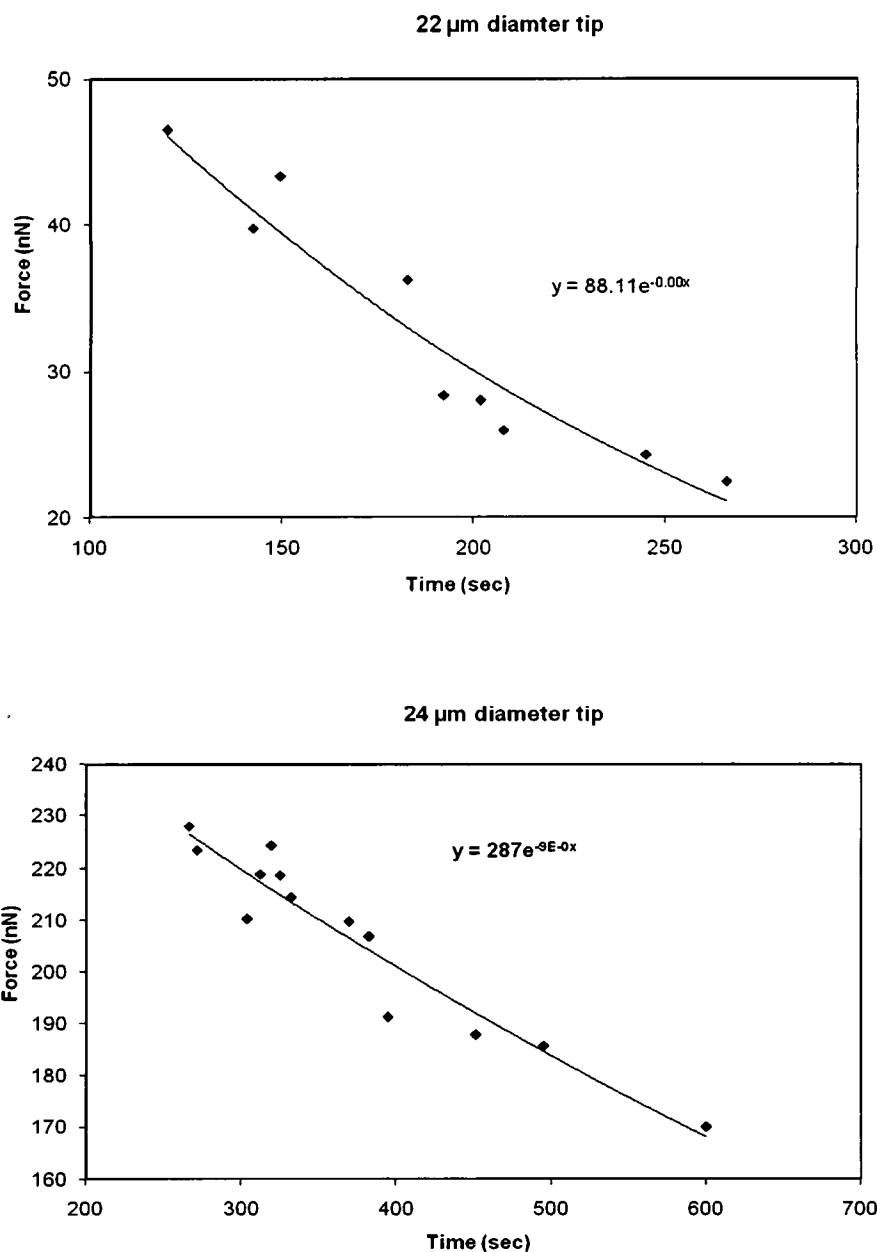


Figure 23: Exponential decay of electrostatic force as a function of time for various $\text{BaF}_2\text{-CaF}_2$ tip diameters

Figure 24 is a plot relating the observed electrostatic force and the z position for three different diameter tips, namely 22 μm , 24 μm and 27 μm . It was observed that the electrostatic force extends beyond 800 nm of probe tip and the substrate separation.

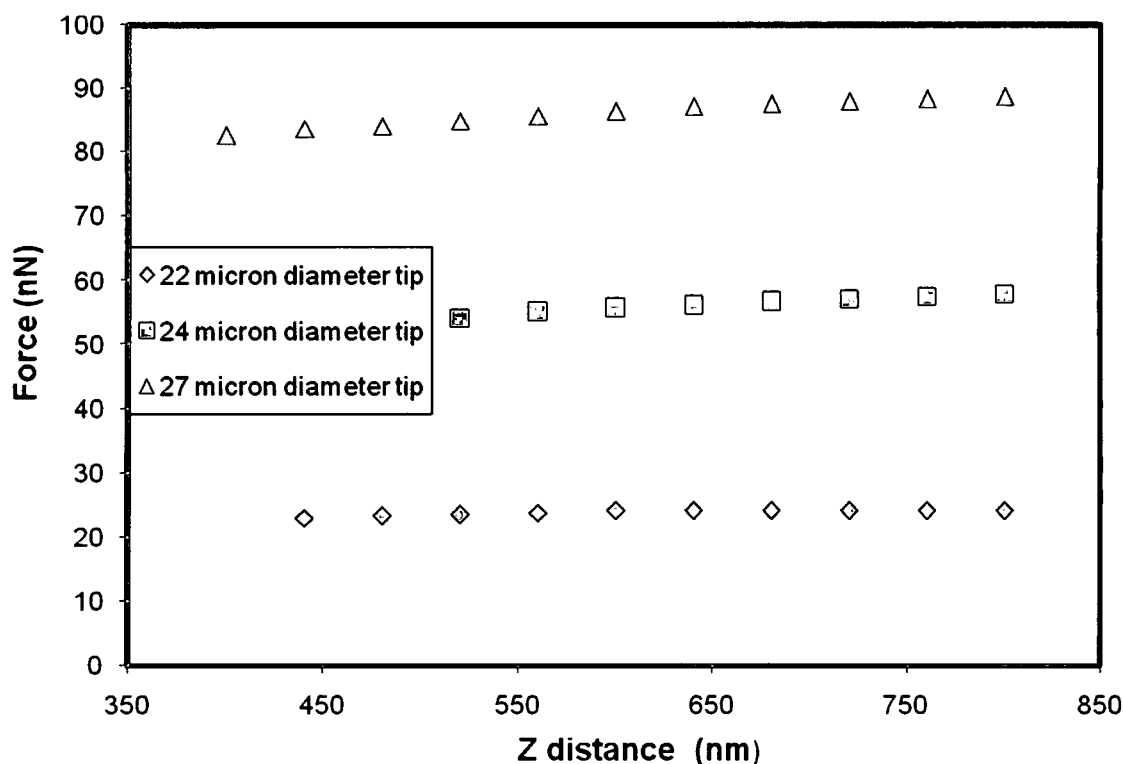


Figure 24: Electrostatic force for several diameter tips of AFM

Tip size can play a major role in the electrostatic force. It was observed that electrostatic force increased with increase in diameter of the tip, being 89 nN for the 27 μm diameter tip and 24 nN for the 22 μm diameter tip. As small size particles contact each other, the electrostatic attraction between them could be more than for different size particles.

3.6) Electrostatic Force Measurement at Various Locations on the Substrate

The eutectic $\text{BaF}_2\text{-CaF}_2$ substrate obtained by high pressure compaction was a pellet shaped substrate with an end to end distance of 7 mm. In order to determine the spatial variability, the force curve was measured from one end to the other end of the substrate. The force curves were obtained at every 0.2 mm distance along the substrate. Figure 25 shows the electrostatic force calculated for 22, 26, and 28 μm diameter tips.

Unlike the previous experiments, these results showed significant variation of force with respect to position. This may be because the force at each location on the substrate will not be the same because of particle size distribution. The particle size of the sample substrate of eutectic $\text{BaF}_2\text{-CaF}_2$ (5 μm - 50 μm), when in contact with the single particle of eutectic $\text{BaF}_2\text{-CaF}_2$ plays an important role in force variation from point to point. The scatter in the electrostatic force was primarily because of roughness of the substrate. To determine the roughness of the substrate, White Light Interferometry was used.

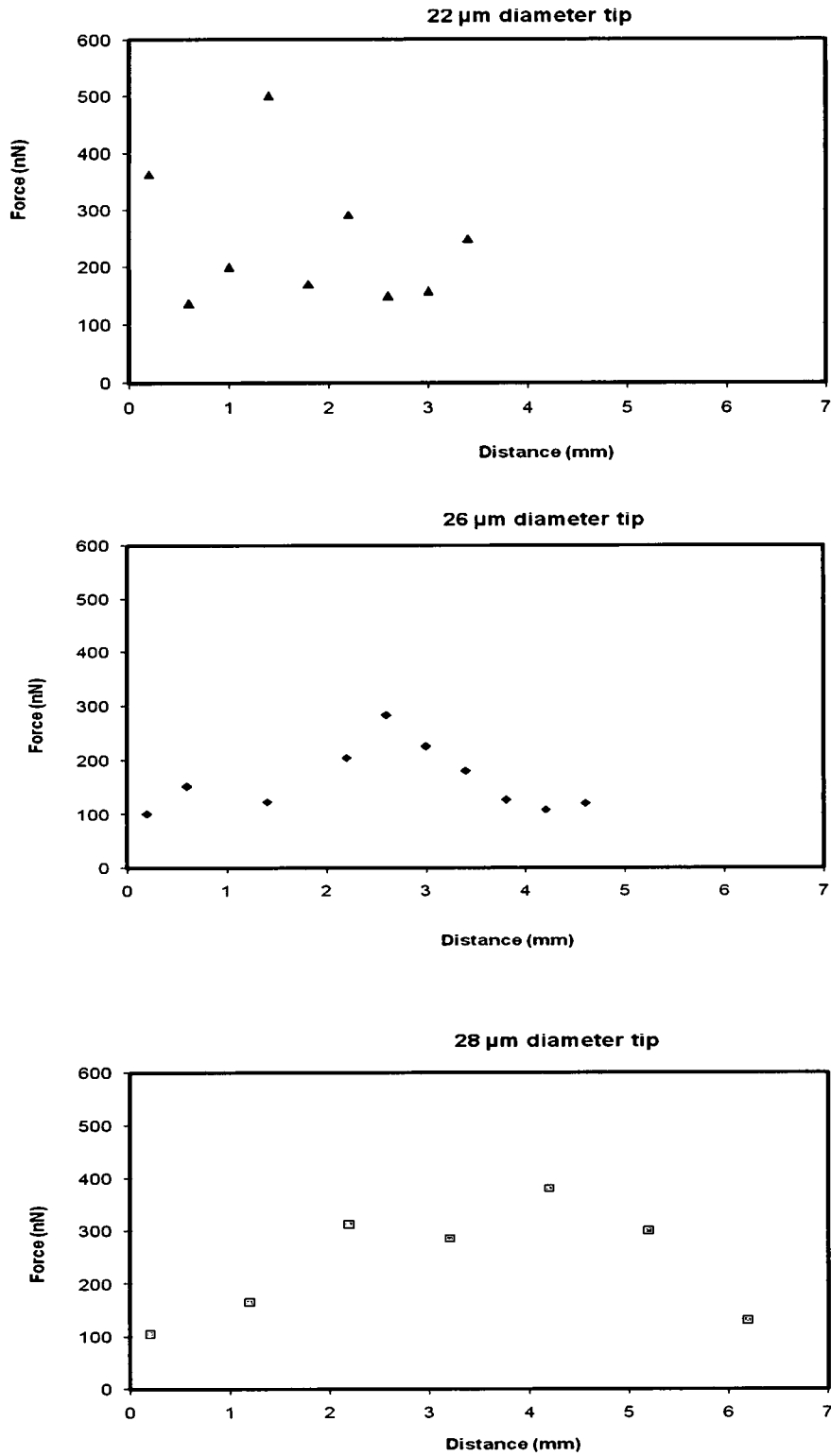


Figure 25: Electrostatic force at various locations on the substrate

3.7) Influence of Particle Roughness on Electrostatic Force Measurement

Asperity plays a major role in the measurement of force. The powder particles of eutectic $\text{BaF}_2\text{-CaF}_2$, being spherical particles, tend to influence the interaction force when it contacts another spherical particle. White light interferometry was used to image the asperity of an individual eutectic $\text{BaF}_2\text{-CaF}_2$ particle (Figure 26). The surface roughness R_q was found to be $10.89\text{ }\mu\text{m}$ for an individual spherical particle of eutectic $\text{BaF}_2\text{-CaF}_2$.

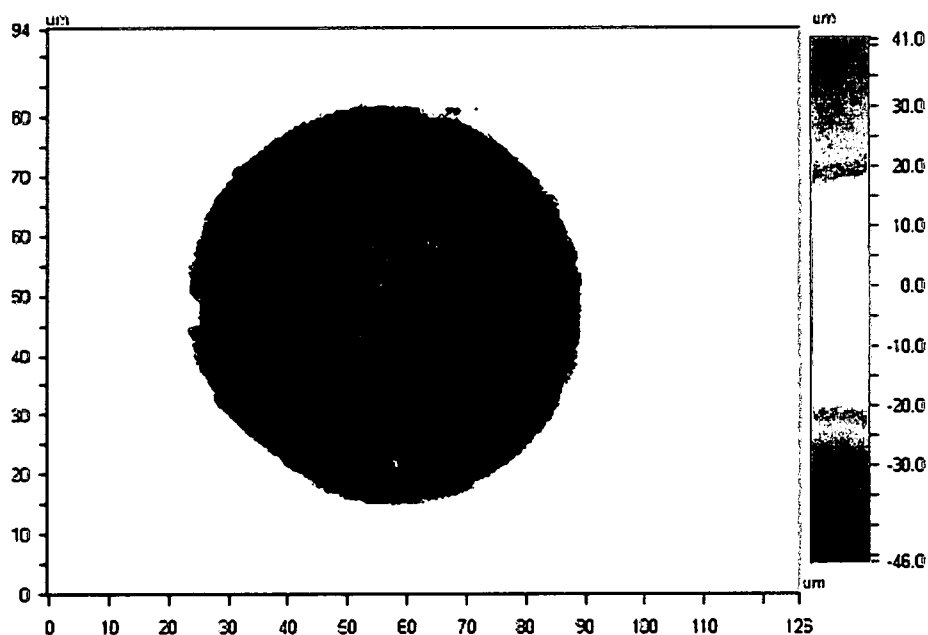
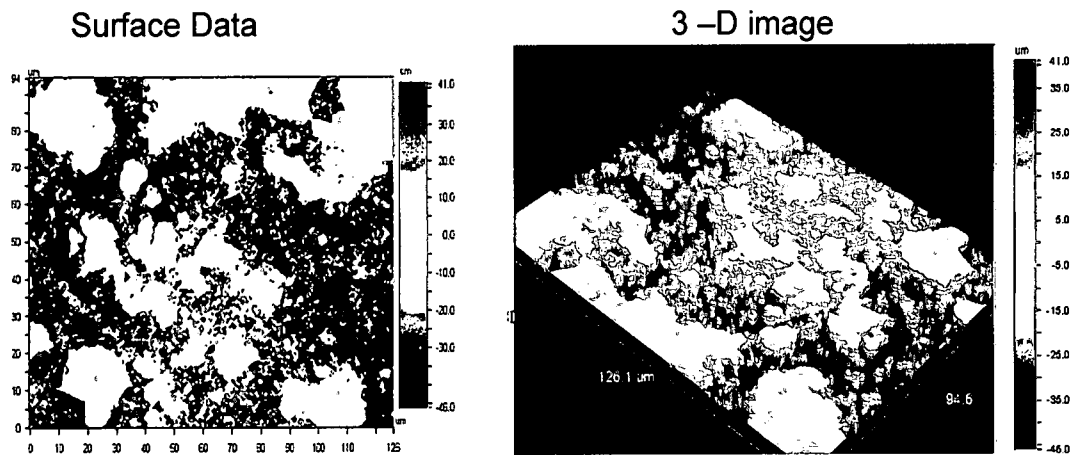
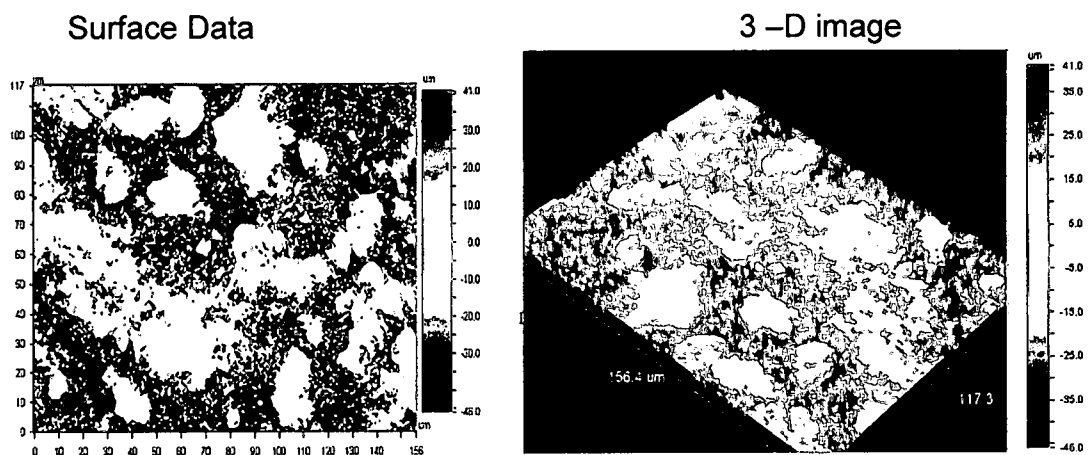


Figure 26: 3-D image showing the asperity of an individual spherical particle of eutectic $\text{BaF}_2\text{-CaF}_2$

Force-distance curves obtained at fixed locations are given as position 1 and position 2. Figure 27 shows the surface topography and 3D image of the substrate for position 1 and position 2. The roughness R_q for position 1 was $2.56\text{ }\mu\text{m}$ and for position 2 was $2.51\text{ }\mu\text{m}$.



Position 1 of the substrate surface



Position 2 of the substrate surface

Figure 27: WLI data of the substrate surface

A stitched image (Figure 28) of eutectic $\text{BaF}_2\text{-CaF}_2$ substrate was obtained by combining the surface data of the substrate for various positions. The overall surface roughness R_q of the stitched image was found to be $3.36\text{ }\mu\text{m}$.

3- D image

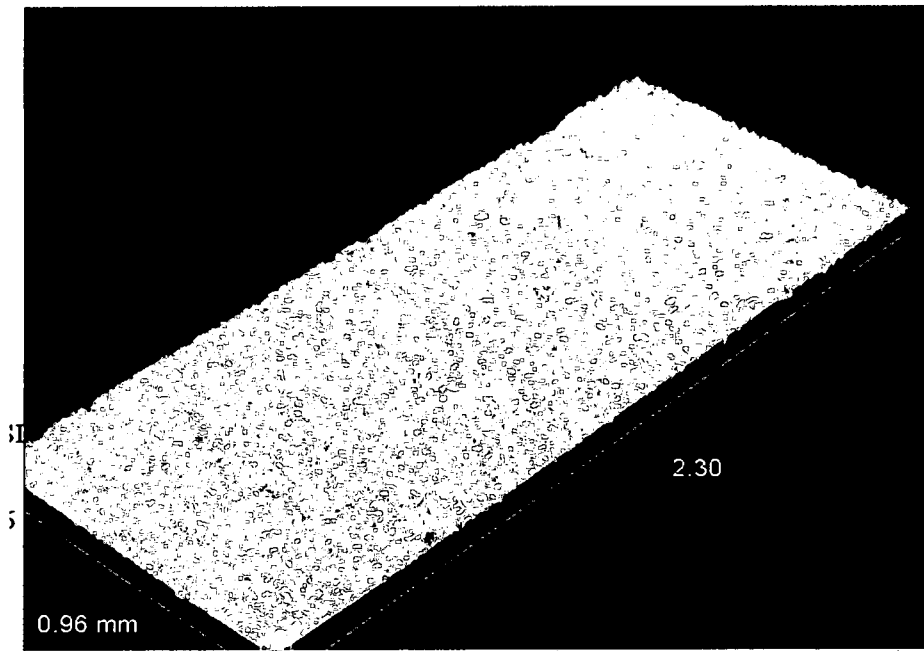


Figure 28: Stitched image of eutectic $\text{BaF}_2\text{-CaF}_2$ substrate

CHAPTER 4

CONCLUSIONS

The objective of the research was to provide guidance to enhance the efficiency of the plasma spray deposition process of solid lubricant coating by determining the role of electrostatic force on the flow properties of eutectic BaF_2 - CaF_2 powder particles. Based on the results of this study, the following observations and conclusions were made.

1. A methodology was developed to create a substrate of eutectic BaF_2 - CaF_2 by compaction at high pressure.
2. A method was developed to electrostatically charge the substrate using an electrostatic generator.
3. An AFM was used for the measurement of electrostatic force and its tip was replaced with a spherical particle of eutectic BaF_2 - CaF_2 . A quantitative electrostatic force between the eutectic BaF_2 - CaF_2 spherical particle and a substrate of eutectic BaF_2 - CaF_2 was measured.
4. The electrostatic force between the eutectic BaF_2 - CaF_2 was found to follow the inverse square behavior of Coulomb's Law.

5. Measurements as a function of the amount of electrostatic charge were compared with measurements performed without charging.
6. The electrostatic force was measured for different diameter tips and it was observed that the force increased with an increase in diameter of the tip.
7. The electrostatic force extends beyond 800 nm and the force was generally observed to be between 20 – 90 nN.
8. In different locations on the substrate, the electrostatic force varies significantly. The variation in the electrostatic force was because of surface roughness, particle size distribution, and protrusions of the spherical particles on the substrate surface.

CHAPTER 5

FUTURE RESEARCH

The following studies are suggested for future research, as this project could not explore all possible avenues due to time and resource restrictions.

The inter-particle forces between eutectic $\text{BaF}_2\text{-CaF}_2$ powder particles used in solid lubricants [PS 304] are affected by the presence of humidity and electrostatic charges. As this study only determined the contribution of electrostatic charge to the interparticle force, the adhesive force between spherical particles of eutectic $\text{BaF}_2 - \text{CaF}_2$ and the substrate of $\text{BaF}_2 - \text{CaF}_2$ as a function of relative humidity can also be investigated.

From the understanding obtained of the relative strength of the measured electrostatic force, new methods can be developed to avoid clogging by eutectic $\text{BaF}_2 - \text{CaF}_2$ particles in plasma spray feed hoppers.

Although this research project was directed towards application to solid lubricants, inter-particle forces are very fundamental to many applications. The understanding gained in this project can be applied in other industries like powder compaction, electrophotography, pharmaceuticals, etc.

REFERENCES

- 1) S. A. Hoenig, "Fine Particles on Semiconductor Surfaces", Removal and Impact on the Semiconductor Industry, K. L. Mittal (Ed.), Vol. 1, pp. 3-16, 1988.
- 2) L. B. Schein, Electrophotography and Development Physics, 2nd ed., Laplacian Press, Morgan Hill, CA, 1996.
- 3) H. Johnson, "Powder Handling and Recovery in the Pharmaceutical Industry", Filtration and Separation, Vol. 33, pp. 787-789, 1996.
- 4) D. A. Hays, "Xerography", G. Trigg (Ed.), Encyclopedia of Applied Physics, Vol. 23, American Institute of Physics, 1998, pp. 541-561.
- 5) J. Q. Feng, D. A. Hays, "Relative Importance of Electrostatic Forces on Powder Particles", Powder Technology, Vol. 135-136, pp. 65-75, 2003.
- 6) J. Q. Feng, "Electrostatic Interaction between Two Charged Dielectric Spheres in Contact", Wilson Center for Research and Technology, NY 14580, Vol. 62, 2000.
- 7) C. DellaCorte, V. Lukaszewicz, M. J. Valco, K. C. Radil and H. Heshmat, "Performance and Durability of High Temperature Foil Air Bearings for Oil-free Turbomachinery", Tribology Transaction, Vol. 43, No. 4, pp. 774-780, 2000.

- 8) C. DellaCorte and J. C Wood, "High Temperature Solid Lubricant Materials for Heavy Duty and Advanced Heat Engines", NASA-TM-106570, National Technical Information Service, Springfield, VA, 1994.
- 9) C. DellaCorte and B. J. Edmonds, "Preliminary Evaluation of PS300", A New Self-Lubricating High Temperature Composite Coating for Use to 800 °C", NASA-tm-107056, National Technical Information Service, Springfield, VA, 1994.
- 10) J. A. Laskowski and DellaCorte, "Friction and Wear Characteristics of Candidate Foil Bearing Materials from 25°C to 800°C", Lubrication Engineering, Vol. 52, pp. 605-12, 1996.
- 11) C. DellaCorte, "Evaluation of Advanced Solid Lubricant Coatings for Foil Bearing Operation at 25°C and 500°C", NASA-TM-206619, National Technical Information Service, Springfield, VA, 1998.
- 12) V. Mangipedi, M. Tirrell, A. V. Pocius, "Direct Measurement of Molecular Level Adhesion Between Poly(Ethylene Terephthalate) and Polyethylene Films, Determination of Surface and Interfacial Energies", J. Adhesion Sci. Technology, Vol. 8, pp. 1251-1270, 1994.
- 13) G. Vigil, Z. Xu, S. Sleinburg and J. Israelachvili, "Interaction of Silica Surface", Journal of Colloid and Interface Science, Vol. 165, pp. 367-385, 1994.
- 14) H. Krupp, "Particle Adhesion: Theory and Experiments", Advances in Colloid and Interface Science, Vol. 1, pp. 111-239, 1967.

- 15) J. N. Israelachvili, "Intermolecular Forces", Colloid Interface Sci., Vol. 44, pp. 255-267, 1973.
- 16) D. Tabor, R. H. S. Winterton, "Force Measurement with Different Spring Constant", Proceedings of the Royal Society of London, Series A, Vol. 312, pp. 435-486, 1969.
- 17) S. Tolansky, "Multiple-Beam Interferometry of Surfaces and Thin Films", Oxford University Press, London, 1984.
- 18) J. L. Parker, H. K. Christenson, B. W. Ninham, "Surface Force Apparatus", Review of Scientific Instruments, Vol. 60, 1978.
- 19) G. Binnig, C.F. Quate and C. Gerber, "Atomic Force Microscope" Physics Review Letters, Vol. 56, pp. 930-933, 1992.
- 20) H. E. Silney, "Solid Lubricants", ASM Handbook, Friction, Lubrication and Wear Technology, Materials Park, OH: ASM International, Vol. 18, 1992.
- 21) B. Bhushan and B. K. Gupta, "Handbook of Tribology: Materials Coating, And Surface Treatment", New York, 1991.
- 22) M. K. Stanford, "Control of Interparticle Cohesion in PS304 Plasma Spray Deposited Solid Lubricant Coating Powder Feedstock", Ph. D. Diss., University of Dayton, 2002.
- 23) M.K. Stanford, C. DellaCorte, D. Eylon, "Effect of Particle Morphology on Flow Characteristics of a Composite Plasma Spray Powders" Journal of Thermal Spray Technology, Vol. 13, pp. 586-592, 2004.

- 24) Y. Y. Tsai, V. Nalladega, S. Sathish and M. K. Stanford, "Evaluation of Interactive Forces between Alkaline Earth Fluoride Particles and Single Crystal Substrate Using Atomic Force Microscopy", Proceedings of SPIE-The International Society for Optical Engineering, 5392, Testing, Reliability, and Application of Micro and Nano Material Systems II, pp. 36-42, 2004.
- 25) B. Bhushan, "Handbook of Nano Technology", Springer-Verlag, New York, 2004.
- 26) K. Michael, J. Hans, and B. Rgen, "The Collidal Probe Technique and its Application to Adhesion Force Measurement", Particle and Particle Characterization, Vol. 19, pp. 129-143, 2002.
- 27) Digital Instruments, Veeco Metrology Group, "Scanning Probe Microscopy Training Notebook", Version 3, 2000.
- 28) H. J. Butt, B. Cappella, M. Kappl, "Force Measurements with the Atomic Microscope Technique, Interpretation and Application", Science Surface Reports, Vol. 59, pp. 1-152, 2005.
- 29) Digital Instruments, Inc. Santa Barbara, CA "Dimensions TM 3000 Scanning Probe Microscope, Instruction Manual", 1996.
- 30) Z. Hongben, G. Martin, and P. Wilfgang, "The Influence of Particle and Roughness on Particle-Substrate Adhesion", Powder Technology, Vol. 135, pp. 82-91, 2003.

2002593630